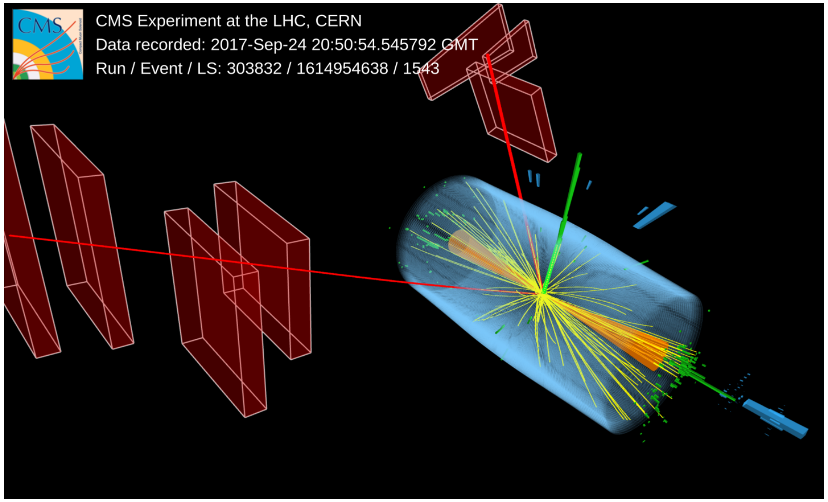

Recent measurements of Vector Boson Scattering at CMS

Brookhaven National Laboratory
Particle Physics Seminar, September, 2020

Aram Apyan

Boson collider

- Vector boson scattering (VBS) at the LHC->colliding bosons
  - Interaction of massive vector bosons (W, Z) radiated by partons of the incoming protons

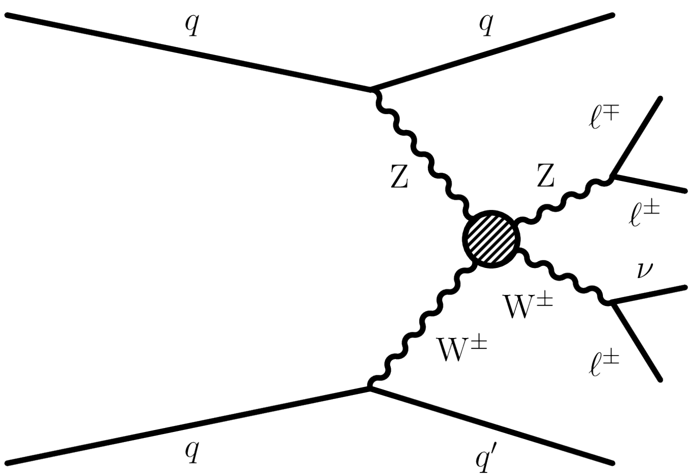

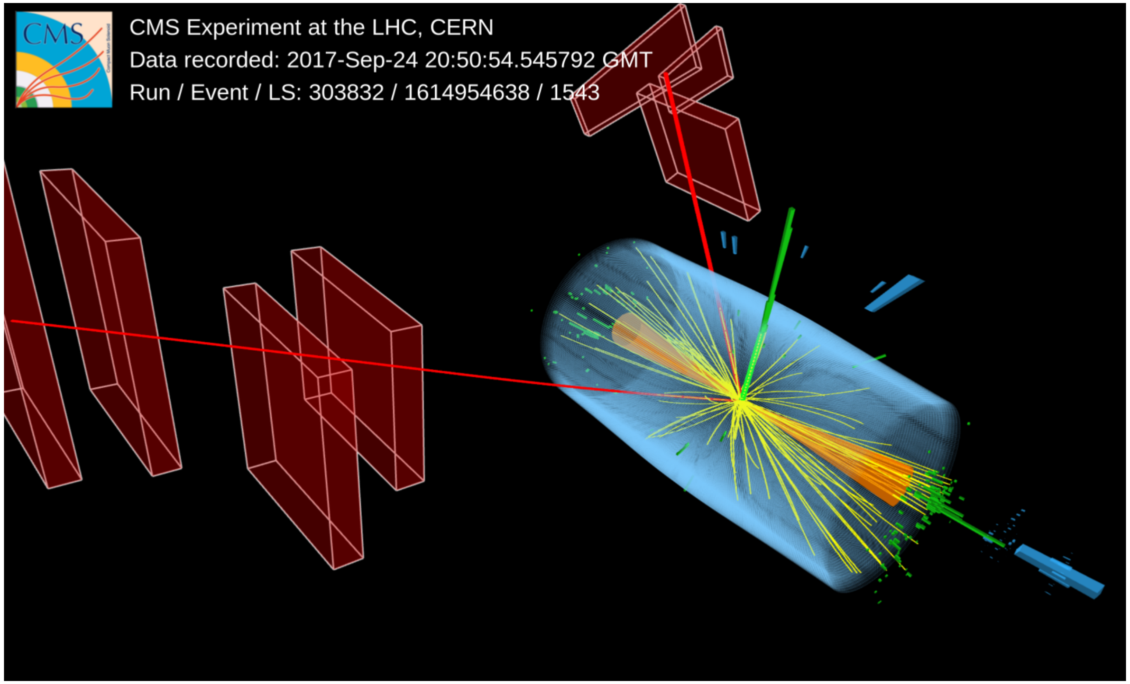

- Signature of VBS events: 2 energetic jets and four fermions
  - Forward jets in opposite hemispheres of the detector
  - Little hadronic activity between the two tagging jets

Gauge boson self-couplings

- W/Z boson self couplings predicted in non-abelian U(1)xSU(2) symmetry
- Quartic gauge couplings (QGC)
  - WWZZ,WWWW,WWZɣ,WWɣɣ
- Triple gauge couplings (TGC)
  - WWZ,WWɣ
- Neutral couplings absent in SM
  - ZZZZ, ZZɣɣ, ZZZ, ZZɣ,…

- **Gauge Interactions**

$$F^a_{\mu\nu} = \partial_\mu A^a_\nu - \partial_\nu A^a_\mu - i g f^a_{bc} A^b_\mu A^c_\nu$$

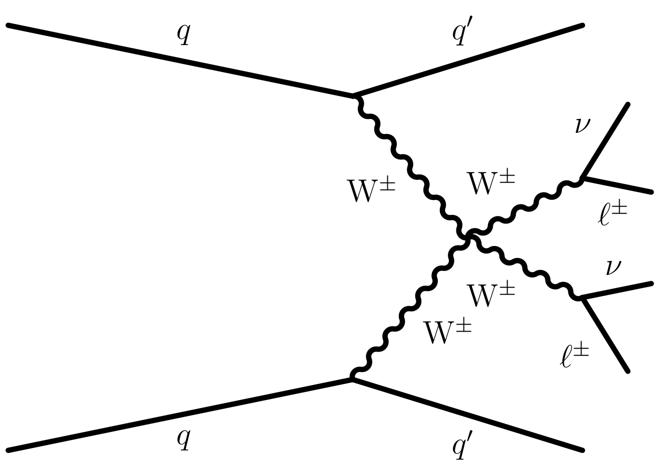

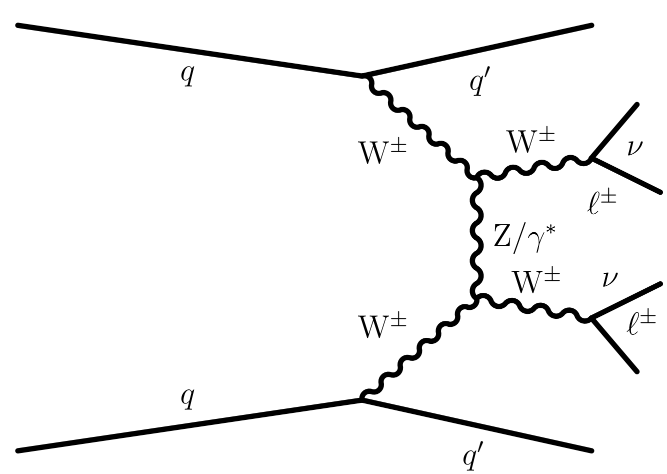

Higgs storyline at the LHC

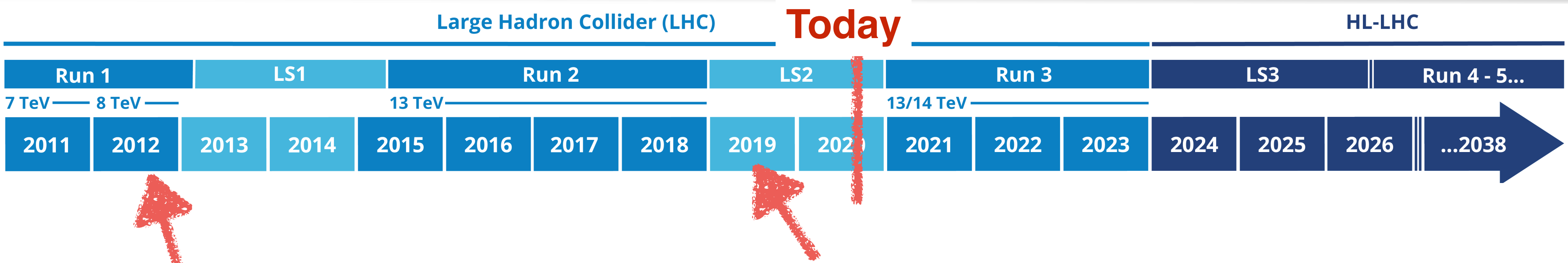

Higgs Boson Discovery

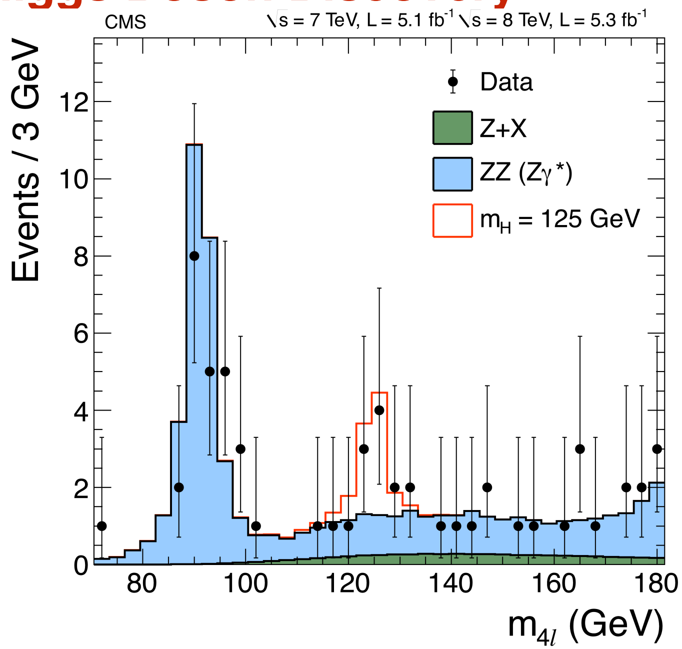

Precision Higgs Physics

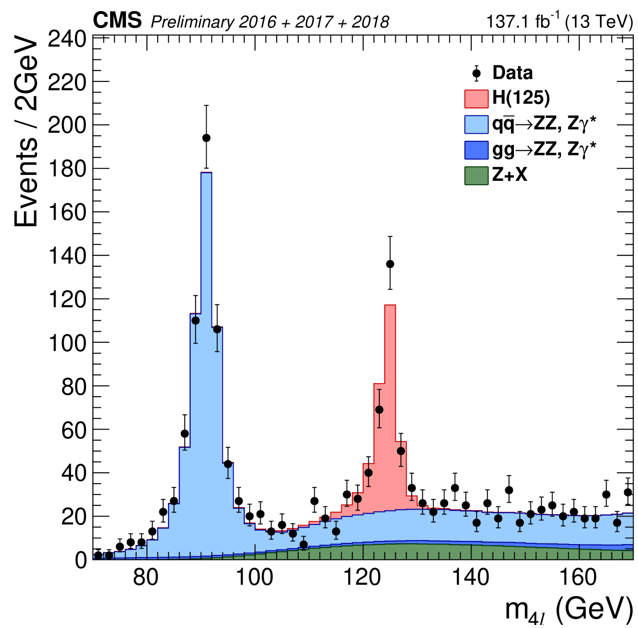

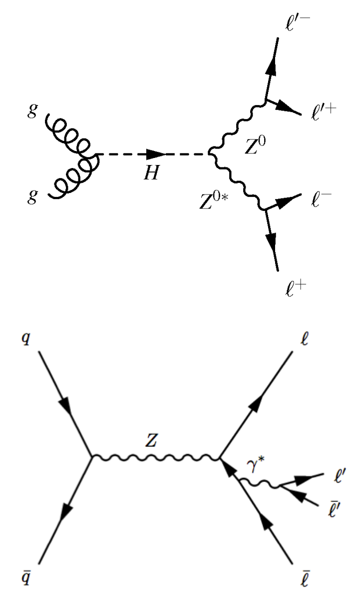

ATLAS CMS Run-1 combination:

$$\boxed{m_{\mathrm{H}} = 125.09 \pm 0.21(\mathrm{stat.}) \pm 0.11(\mathrm{syst.})\ \mathrm{GeV}}$$

Higgs Physics

- Cornerstone of the LHC physics
  - Post discovery: The Higgs boson as a tool for discovery
  - Standard Model (SM)-like Higgs so far

- Many open questions and opportunities
  - Are observations fully consistent with the SM picture?
  - Interactions with SM particles
  - Interactions with new particles (including Higgs as portal to Dark Matter)
  - Higgs self interactions
  - Role of the Higgs boson in vector boson scattering
  - Extended Higgs sector

Electroweak Multiboson measurements

- Test of the electroweak (EW) sector of Standard Model (SM) at TeV scale
  - Scattering of massive weak gauge bosons
  - Probe the nature of EW symmetry breaking
    - Complimentary to direct Higgs boson measurements

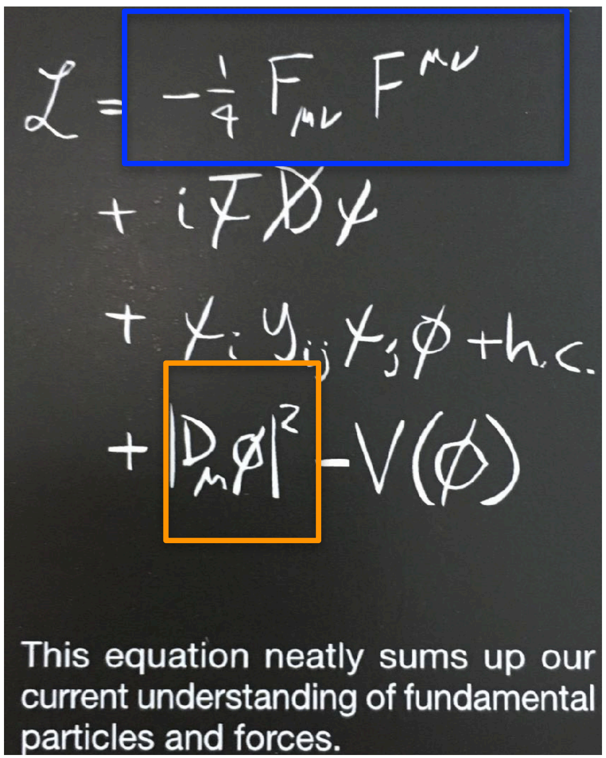

- e.g. WWWW, WWZ

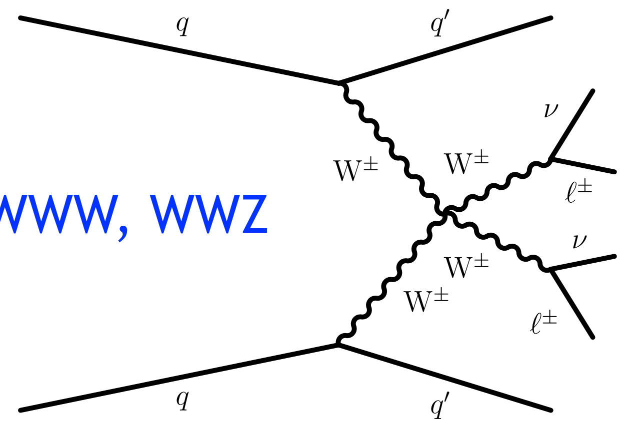

- e.g., HWW, HZZ

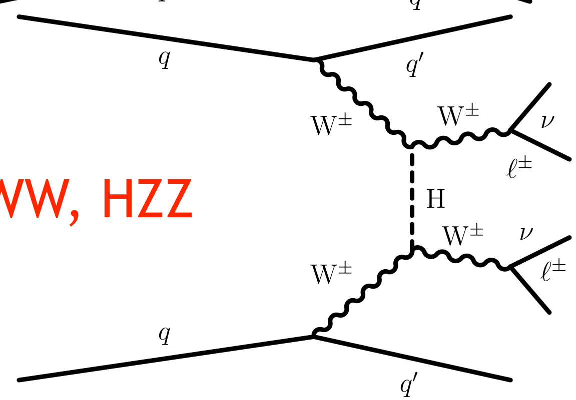

Interplay with perturbative unitarity

- First experimental evidence of self couplings at LEP2 experiment

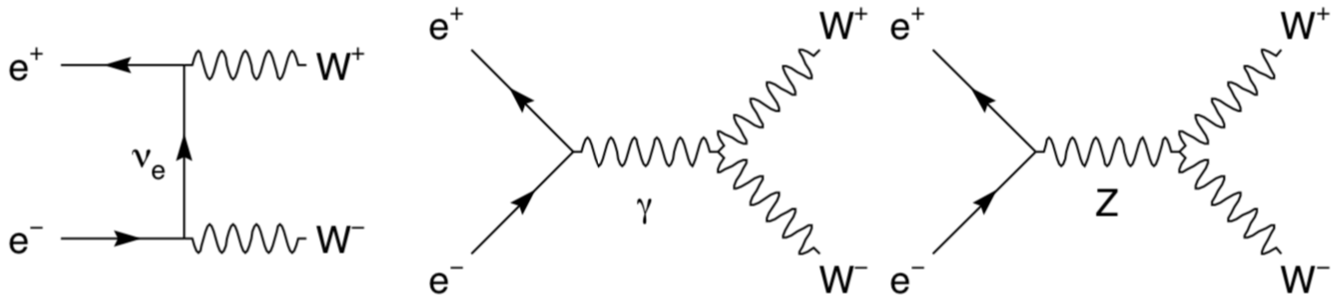

- Without WWZ vertex
  - Cross section grows with energy
  - Unitarity is violated
    - Probability not conserved
- Unitarity problem 'fixed' by Z boson
  - Confirmation of WWZ vertex

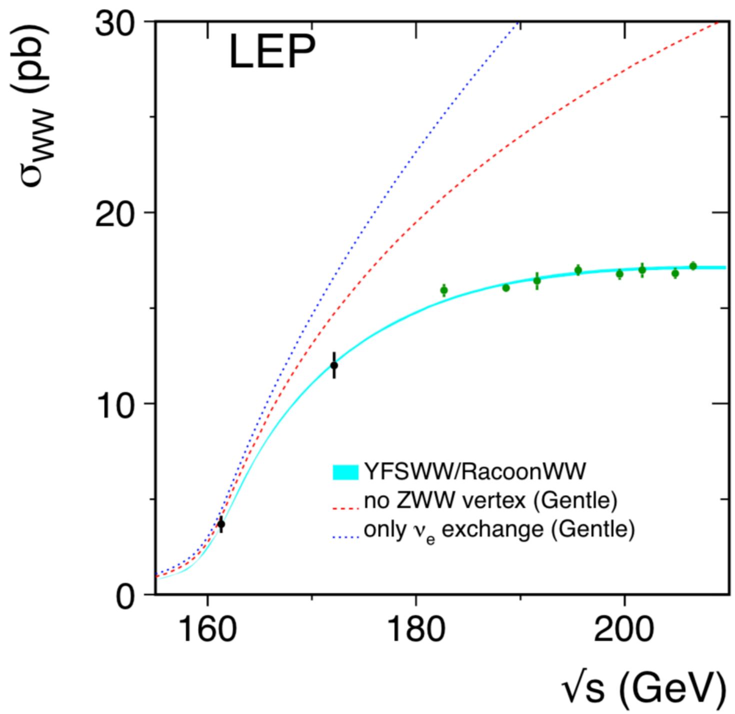

VBS and unitarity

- Heavy vector bosons W and Z acquire their mass and longitudinal polarization state through Higgs mechanism
- Consider the cross section of the longitudinal scattering $W_LW_L \to W_LW_L$

$$\epsilon^{\mu}_{T_1,T_2} = \frac{1}{\sqrt{2}}(0,1,\pm i,0) \quad \Big| \quad \epsilon^{\mu}_{L} = \frac{1}{m}(k_3,0,0,E)$$

$$\mathcal{A}(W_LW_L \to W_LW_L) \propto \frac{g_W^2}{v^2}\Big[-s-t+$$

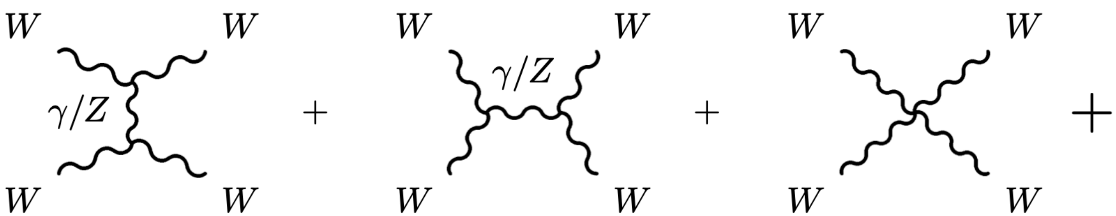

VBS and unitarity

- Heavy vector bosons W and Z acquire their mass and longitudinal polarization state through Higgs mechanism
- Consider the cross section of the longitudinal scattering $W_LW_L \to W_LW_L$

$$\epsilon^{\mu}_{T_1,T_2} = \frac{1}{\sqrt{2}}(0,1,\pm i,0) \quad \Big| \quad \epsilon^{\mu}_{L} = \frac{1}{m}(k_3,0,0,E)$$

$$\mathcal{A}(W_LW_L \to W_LW_L) \propto \frac{g_W^2}{v^2}\left[-s-t+\frac{s^2}{s-m_H^2}+\frac{t^2}{t-m_H^2}\right]$$

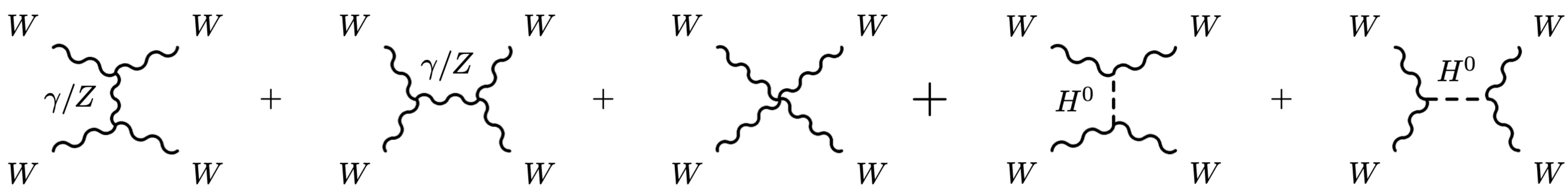

VBS and unitarity

- Heavy vector bosons W and Z acquire their mass and longitudinal polarization state through Higgs mechanism
- Consider the cross section of the longitudinal scattering $W_LW_L \to W_LW_L$

$$\epsilon^{\mu}_{T_1,T_2} = \frac{1}{\sqrt{2}}(0,1,\pm i,0) \;\Big|\; \epsilon^{\mu}_{L} = \frac{1}{m}(k_3,0,0,E)$$

$$-g_W^2 \frac{M_H^2}{4M_W^2}\left[\frac{s}{s-M_H^2}+\frac{t}{t-M_H^2}\right], \text{with } s = 4E^2$$

well-behaved at high energies ($s \to \infty$)

- A SM Higgs boson exactly cancels the increase at large energies
- The amplitude may still violate unitarity for large Higgs mass

VBS and Higgs

PHYSICAL REVIEW D VOLUME 16, NUMBER 5 1 SEPTEMBER 1977

Weak interactions at very high energies: The role of the Higgs-boson mass

Benjamin W. Lee,* C. Quigg,† and H. B. Thacker
Fermi National Accelerator Laboratory,‡ Batavia, Illinois 60510

(Received 20 April 1977)

We give an S-matrix-theoretic demonstration that if the Higgs-boson mass exceeds $M_c = (8\pi\sqrt{2}/3G_F)^{1/2}$, parital-wave unitarity is not respected by the tree diagrams for two-body scattering of gauge bosons, and the weak interactions must become strong at high energies. We exhibit the relation of this bound to the structure of the Higgs-Goldstone Lagrangian, and speculate on the consequences of strongly coupled Higgs-Goldstone systems. Prospects for the observation of massive Higgs scalars are noted.

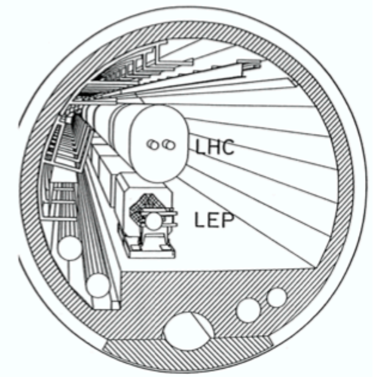

LARGE HADRON COLLIDER
IN THE LEP TUNNEL
Vol. I

11. SUMMARY AND CONCLUSIONS

A theoretical consensus is emerging that new phenomena will be discovered at or below 1 TeV. There is no consensus about the nature of these phenomena but it is interesting that many of the ideas which have been suggested can be tested in experiments at an LHC. Although many, if not all, of these ideas will doubtless have been discarded, disproved or established by the time an LHC is built, this demonstrates the potential virtues of such a machine.

- Lee-Quigg-Thacker bound:

$$\boxed{M_H^{\,2} \le \frac{8\pi\sqrt{2}}{3G_F} \equiv M_c^{\,2} \simeq (1\ \mathrm{TeV}/c^2)^2}$$

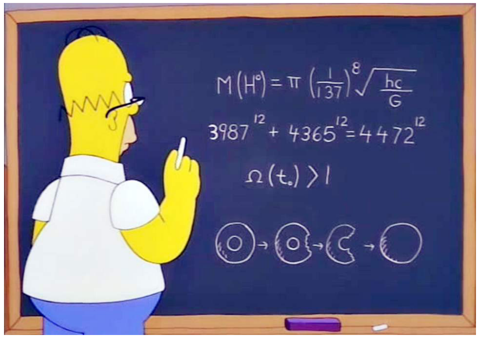

VBS and Higgs

- The MH=125 GeV Higgs will unitarize VV->VV scattering provided is has SM hVV couplings!
- Measurements of VBS after the Higgs discovery
    - Probes the Higgs VV couplings
        - Significant excess in the longitudinally polarized channel would point to new interactions in the EW sector
    - Complementary to measurements of H->VV decays

SM without a Higgs boson

SM with a 120 GeV Higgs boson

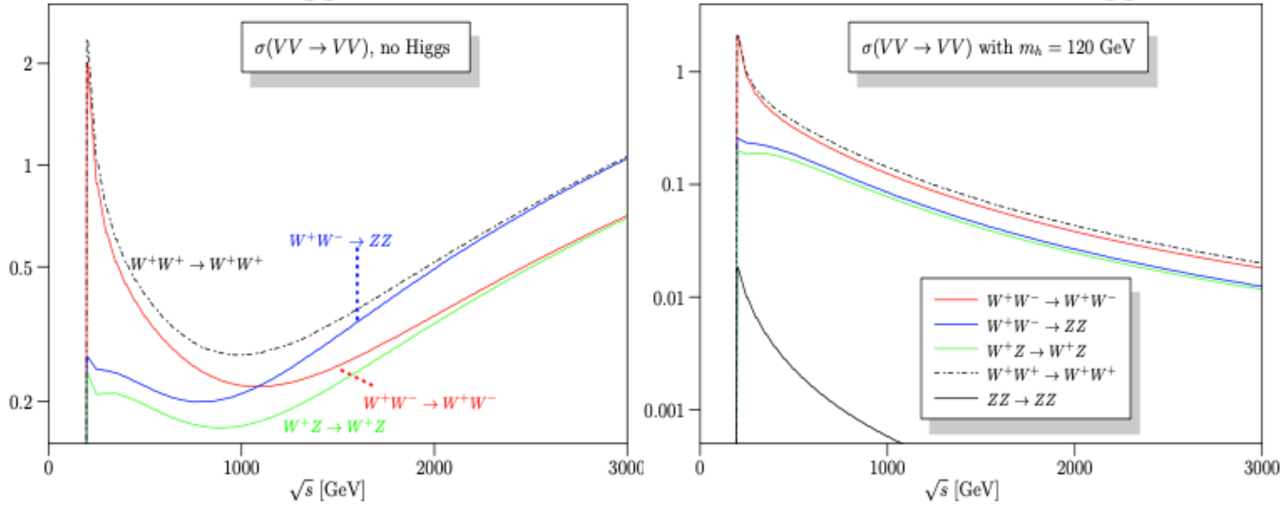

from ArXiv:0806.4145

CMS Run 2 datasets

- Cross sections of VBS final states: O(1 fb)
- Large dataset available at 13 TeV
  - About 140 fb^{-1} recorded

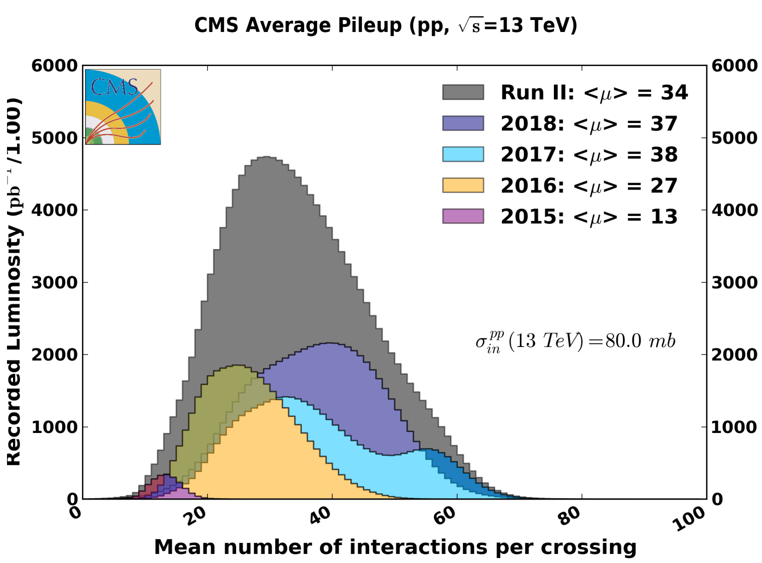

	CMS	$\sqrt{s}$ [TeV]	L [fb^{-1}]
Run I	2010	7	0.045
	2011	7	6
	2012	8	23
Run II	2015	13	4
	2016	13	41
	2017	13	51
	2018	13	68
Run III	2021	14	10-20
	2022	14	60
	2023	14	90
	2024 ?	14	80
	2027-2038	14	3000

VV scattering at LHC

- VVjj process cross section at leading-order (LO):
  - Pure EW contribution at $O(\alpha^6)$ with VBS forming an important subclass
    - Also includes irreducible EW contributions (separately not gauge-invariant)

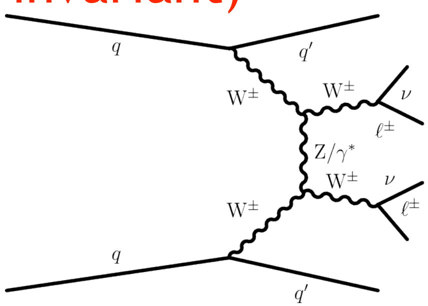

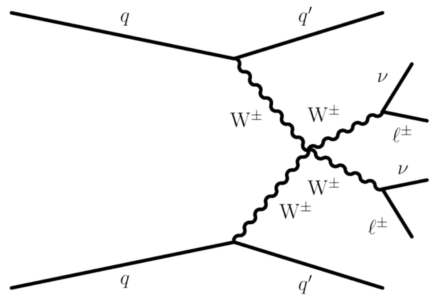

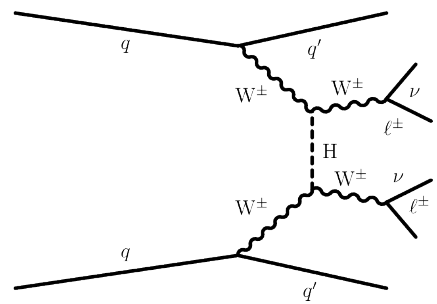

  - QCD induced contribution at $O(\alpha^4\alpha_s^2)$

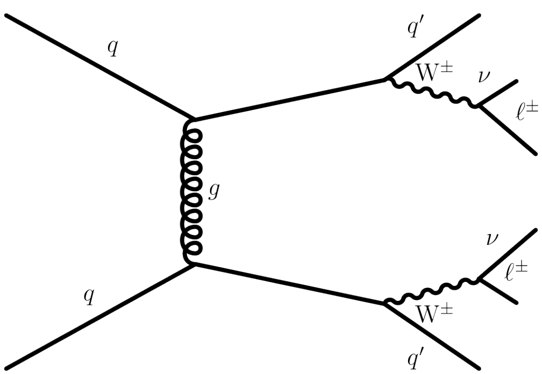

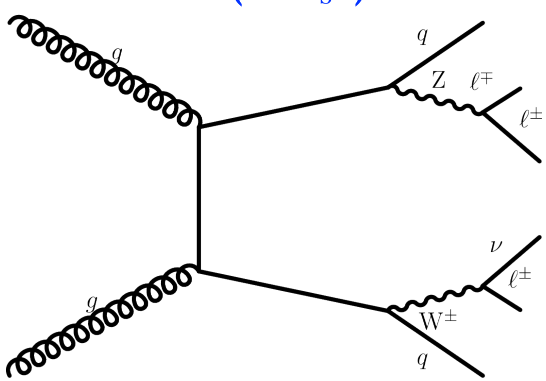

  - Small interference of the EW and QCD amplitudes at $O(\alpha^5\alpha_s)$

Same-sign WW and WZ measurement

- First simultaneous $W^{\pm}W^{\pm}jj$ and WZjj production cross section measurements using fully leptonic final states (electrons and muons) ArXiv:2005.01171
  - Measure EW and EW+QCD production for $W^{\pm}W^{\pm}jj$ production
  - Measure EW, QCD, and EW+QCD production for WZjj
- $W^{\pm}W^{\pm}$ has the largest ratio of EW production to QCD initiated production
  - Double charge structure of the leptonic final state
  - Small QCD WW (no diagrams with initial state gluon-gluon or quark-gluon)
- WZjj is a clean channel with three leptons
  - Use machine learning to discriminate EW and QCD production
- Analysis strategy: simultaneous fit in the $W^{\pm}W^{\pm}$ and WZ signal regions and control regions to measure normalization of main background processes in situ
  - Nonprompt lepton, charge-misidentification, tZq, and other background processes

Same-sign WW

- Observed number of events consistent with SM predictions
  - Dijet mass (left) and dilepton mass (right) distributions used in the fit
  - LO Madgraph is used to simulate the $W^{\pm}W^{\pm}jj$ process

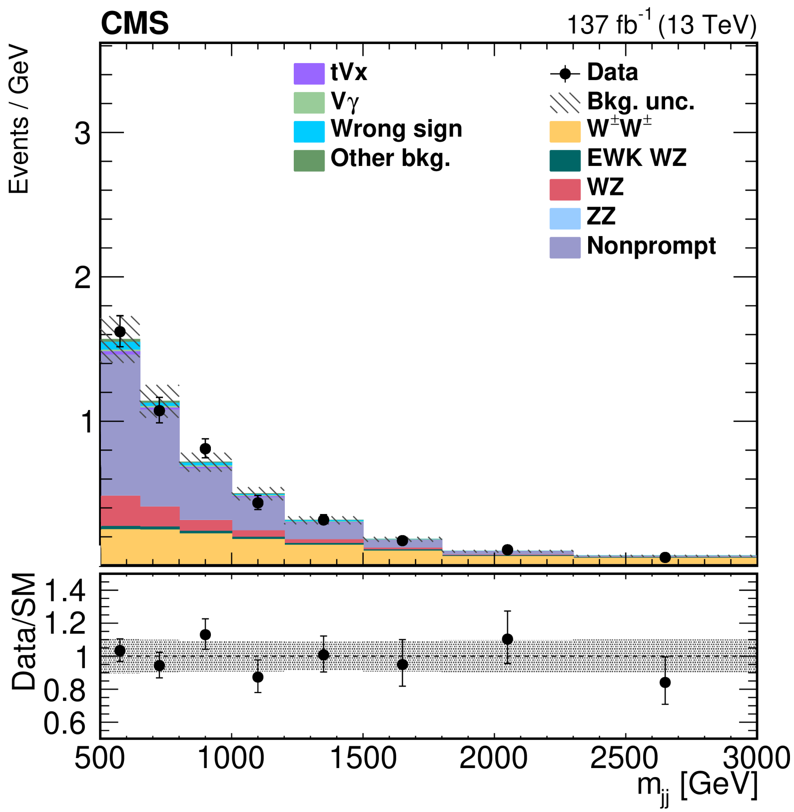

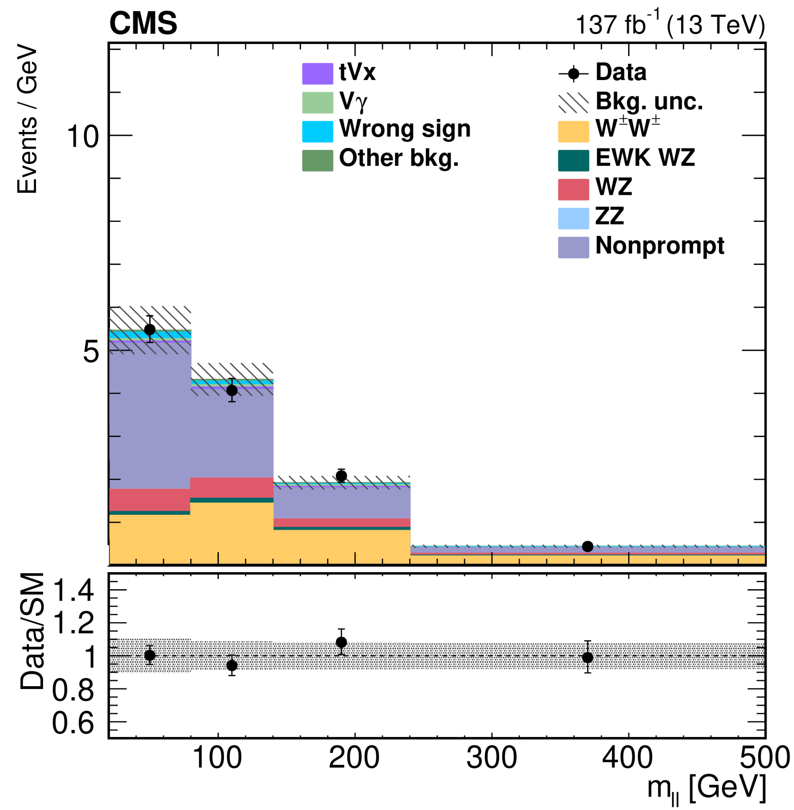

Observation of EW WZ process at CMS

- Dijet mass and boosted decision tree (used in the fit) distributions
- EW WZ observed (expected from Madgraph LO prediction) statistical significance of 6.8 (5.3) standard deviations

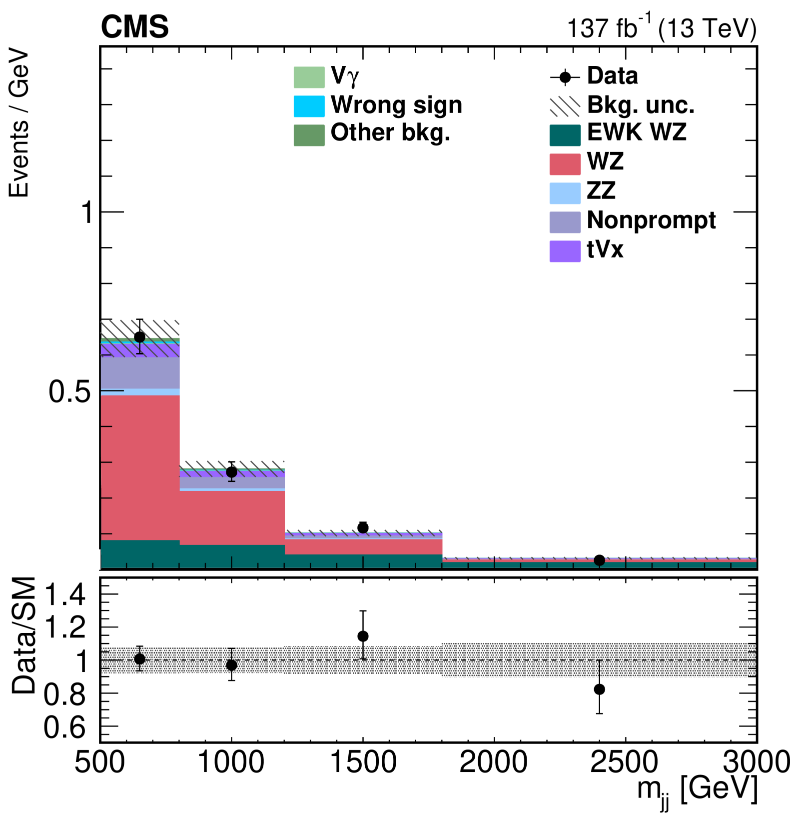

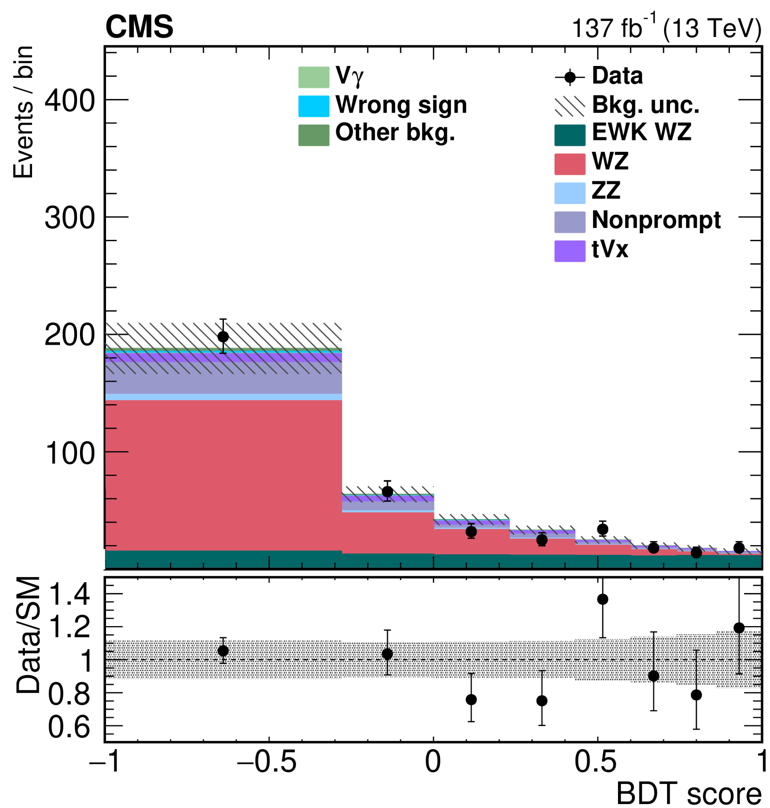

Distributions in WW/WZ signal region

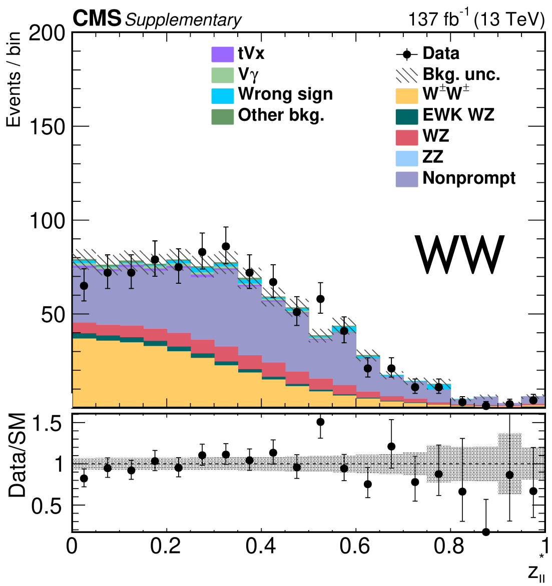

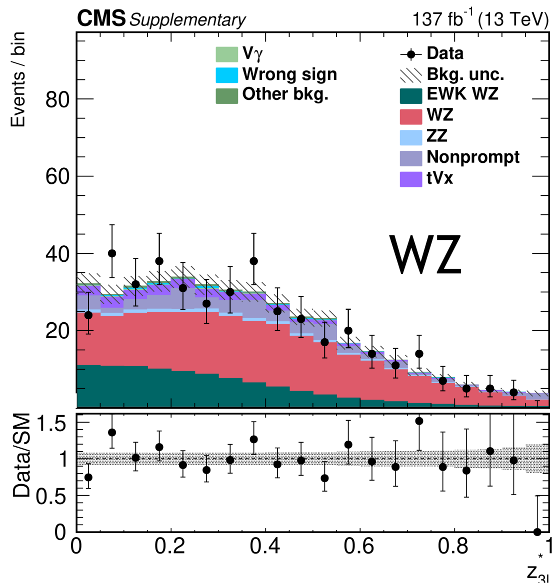

Zeppenfeld variable

$$z^*_\ell = \left|\eta^\ell - \frac{\eta^{j_1} + \eta^{j_2}}{2}\right| / |\Delta\eta_{jj}|$$

Phys. Rev. D 54 (1996) 6680

Good agreement between data and prediction

Δϕ of the two jets

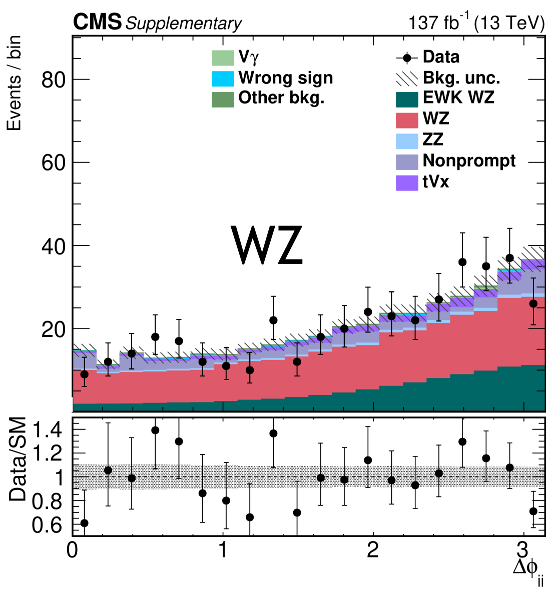

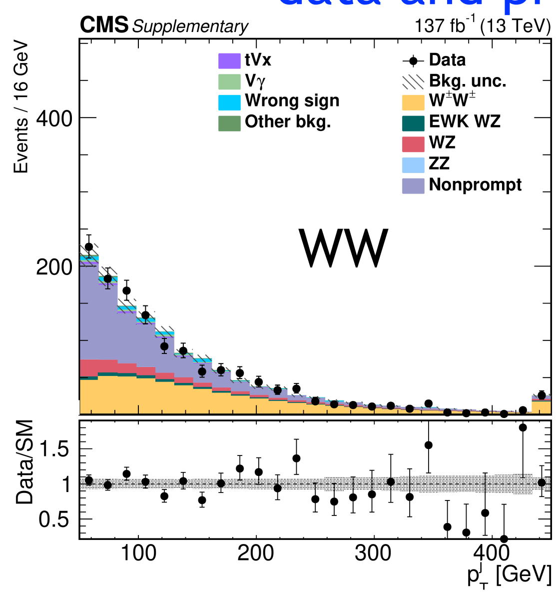

p_T of jets

Inclusive fiducial cross sections

- Measurements compatible with predictions within uncertainties

$W^{\pm}W^{\pm}$ fiducial region:

- two same-sign leptons with $p_T > 20\mathrm{GeV}$, $|\eta| < 2.5$, and $m_{\ell\ell} > 20\mathrm{GeV}$
- two jets with $m_{jj} > 500\mathrm{GeV}$ and $|\Delta\eta_{jj}| > 2.5$

WZ fiducial region:

- three leptons with $p_T > 20\mathrm{GeV}$, $|\eta| < 2.5$, and a pair of opposite charge same-flavor lepton pair $|m_{\ell\ell} - m_Z| < 15\mathrm{GeV}$
- two jets with $m_{jj} > 500\mathrm{GeV}$ and $|\Delta\eta_{jj}| > 2.5$

Process	$\sigma\mathcal{B}$ (fb)	Theoretical prediction without NLO corrections (fb)	Theoretical prediction with NLO corrections (fb)
EW $W^{\pm}W^{\pm}$	3.98 ± 0.45 $0.37\,(\mathrm{stat}) \pm 0.25\,(\mathrm{syst})$	3.93 ± 0.57	3.31 ± 0.47
EW+QCD $W^{\pm}W^{\pm}$	4.42 ± 0.47 $0.39\,(\mathrm{stat}) \pm 0.25\,(\mathrm{syst})$	4.34 ± 0.69	3.72 ± 0.59
EW WZ	1.81 ± 0.41 $0.39\,(\mathrm{stat}) \pm 0.14\,(\mathrm{syst})$	1.41 ± 0.21	1.24 ± 0.18
EW+QCD WZ	4.97 ± 0.46 $0.40\,(\mathrm{stat}) \pm 0.23\,(\mathrm{syst})$	4.54 ± 0.90	4.36 ± 0.88
QCD WZ	3.15 ± 0.49 $0.45\,(\mathrm{stat}) \pm 0.18\,(\mathrm{syst})$	3.12 ± 0.70	3.12 ± 0.70

Systematic uncertainties

Source of uncertainty	$W^{\pm}W^{\pm}$ (%)	WZ (%)
Integrated luminosity	1.5	1.6
Lepton measurement	1.8	2.9
Jet energy scale and resolution	1.5	4.3
Pileup	0.1	0.4
b tagging	1.0	1.0
Nonprompt rate	3.5	1.4
Trigger	1.1	1.1
Limited MC sample size	2.6	3.7
Theory	1.9	3.8
Total systematic uncertainty	5.7	7.9
Statistical uncertainty	8.9	22
Total uncertainty	11	23

* Limited MC sample size->includes limited number of data events used to estimate nonprompt lepton background

Higher order corrections

- Same sign WW is the only diboson process with full NLO computation (EW and QCD)

$$
\begin{tikzcd}[column sep=small]
\textbf{LO} & & \mathcal{O}(\alpha^6) \arrow[dl, "\mathrm{EW}"'] \arrow[dr, "\mathrm{QCD}"] & & \mathcal{O}(\alpha_s\alpha^5) \arrow[dl, "\mathrm{EW}"'] \arrow[dr, "\mathrm{QCD}"] & & \mathcal{O}(\alpha_s^2\alpha^4) \arrow[dl, "\mathrm{EW}"'] \arrow[dr, "\mathrm{QCD}"] & \\
\textbf{NLO} & \mathcal{O}(\alpha^7) & & \mathcal{O}(\alpha_s\alpha^6) & & \mathcal{O}(\alpha_s^2\alpha^5) & & \mathcal{O}(\alpha_s^3\alpha^4)
\end{tikzcd}
$$

ArXiv:1611.02951
ArXiv:1708.00268
ArXiv:1904.00882
ArXiv:2009.00411

Order	$\mathcal{O}(\alpha^7)$	$\mathcal{O}(\alpha_s\alpha^6)$	$\mathcal{O}(\alpha_s^2\alpha^5)$	$\mathcal{O}(\alpha_s^3\alpha^4)$	Sum
$\delta\sigma_{\mathrm{NLO}}$ [fb]	$-0.2169(3)$	$-0.0568(5)$	$-0.00032(13)$	$-0.0063(4)$	$-0.2804(7)$
$\delta\sigma_{\mathrm{NLO}}/\sigma_{\mathrm{LO}}$ [%]	-13.2	-3.5	0.0	-0.4	-17.1

- EW corrections are large and negative (~-15%) in the fiducial region
    - Similar large EW corrections for the WZ and ZZ(new) processes
    - Corrections increase in magnitude with increasing dilepton/dijet masses
- Meaningless distinction between EW signal and QCD background at NLO

Differential measurements

- Detailed characterization of the WW production
  - Consistent picture with the SM!
  - Absolute and normalized cross section measurements
  - Measurements compared to LO Madgraph predictions (blue) and predictions with NLO corrections (red)

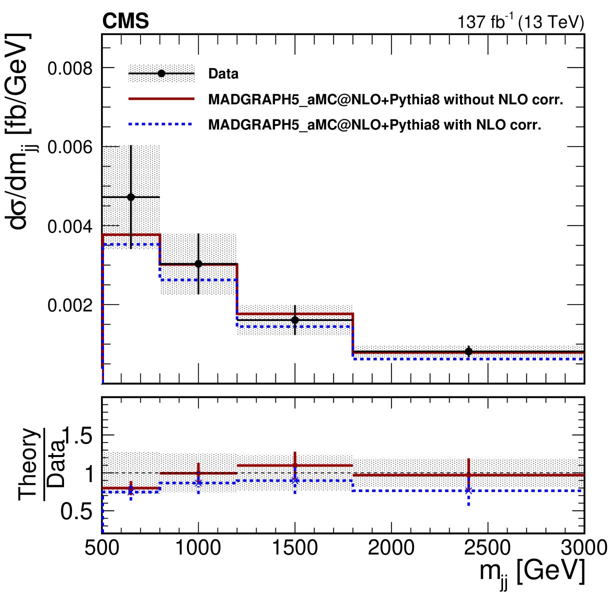

Dijet mass

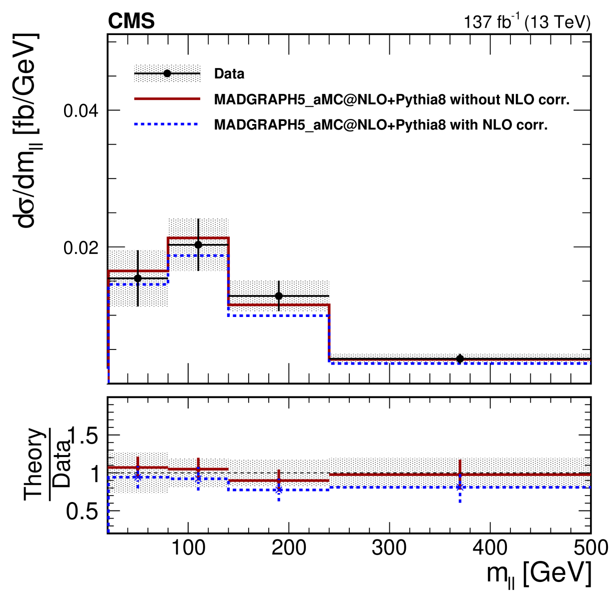

Dilepton mass

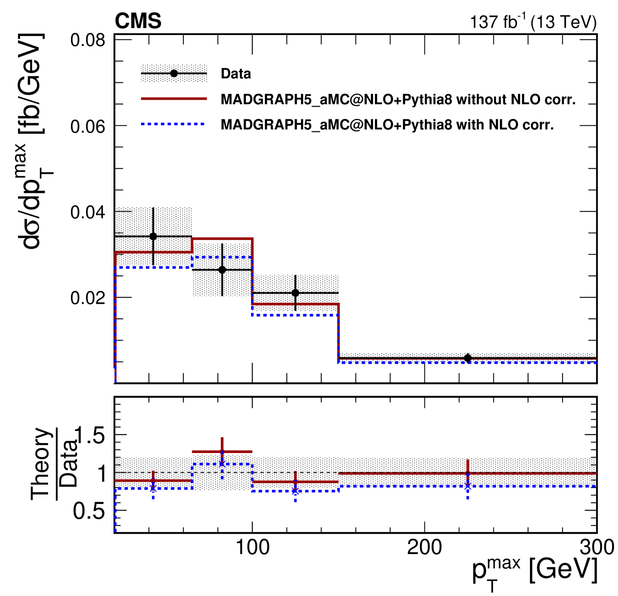

Leading lepton p_T

Differential measurements

- WZ fiducial cross section measurement as function of dijet mass (m_{jj})
  - Agreement between measured and predicted cross sections
  - m_{jj} measurement performed by replacing the BDT with m_{jj} in the fit

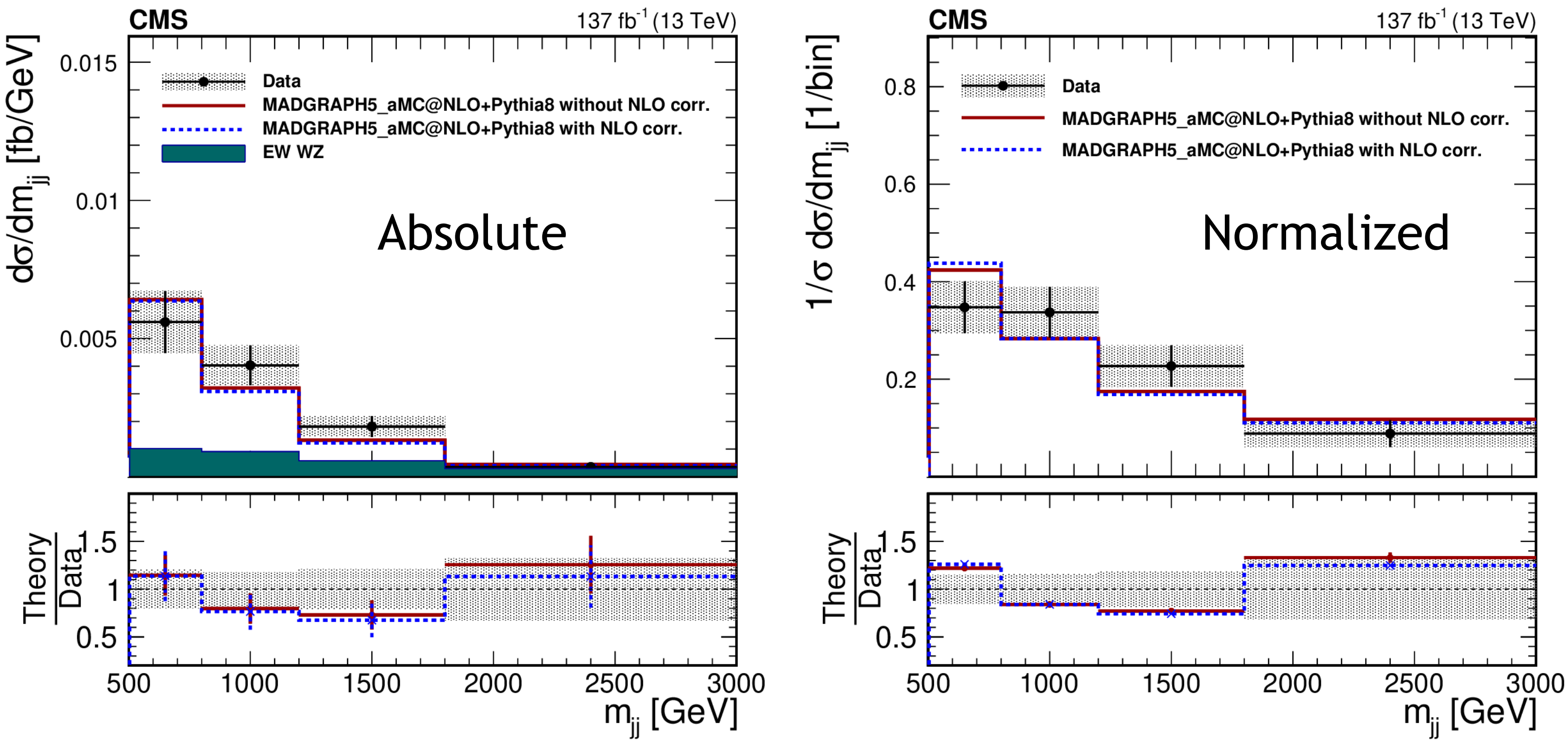

EW ZZ production

- Measurement of EW ZZjj production using four lepton final state
  - Very clean data sample with rather small non-ZZ background
    - Low signal yield -> lepton selection as efficient as possible
  - Relatively large QCD ZZ contribution
- Making us of a matrix-element discriminant (K_D) to enhance EW production
  - The details can be found in Arxiv:1309.4819

- Visible excess of data events consistent with EW ZZ contribution

- Observed (expected) statistical Significance of 4.0 (3.5) standard deviations

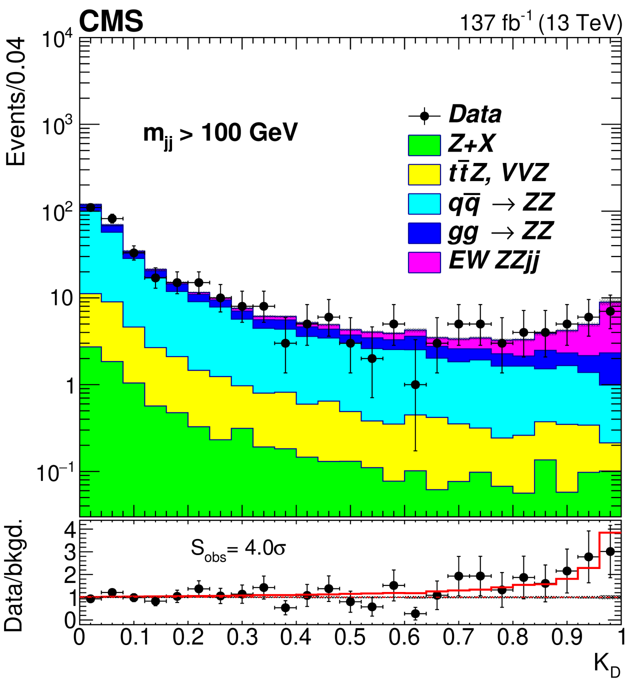

Longitudinal scattering and Higgs

- What about the longitudinal scattering?
  - Extremely challenging as the $W_LW_L \to W_LW_L$ is ~10% of the total WW scattering cross section

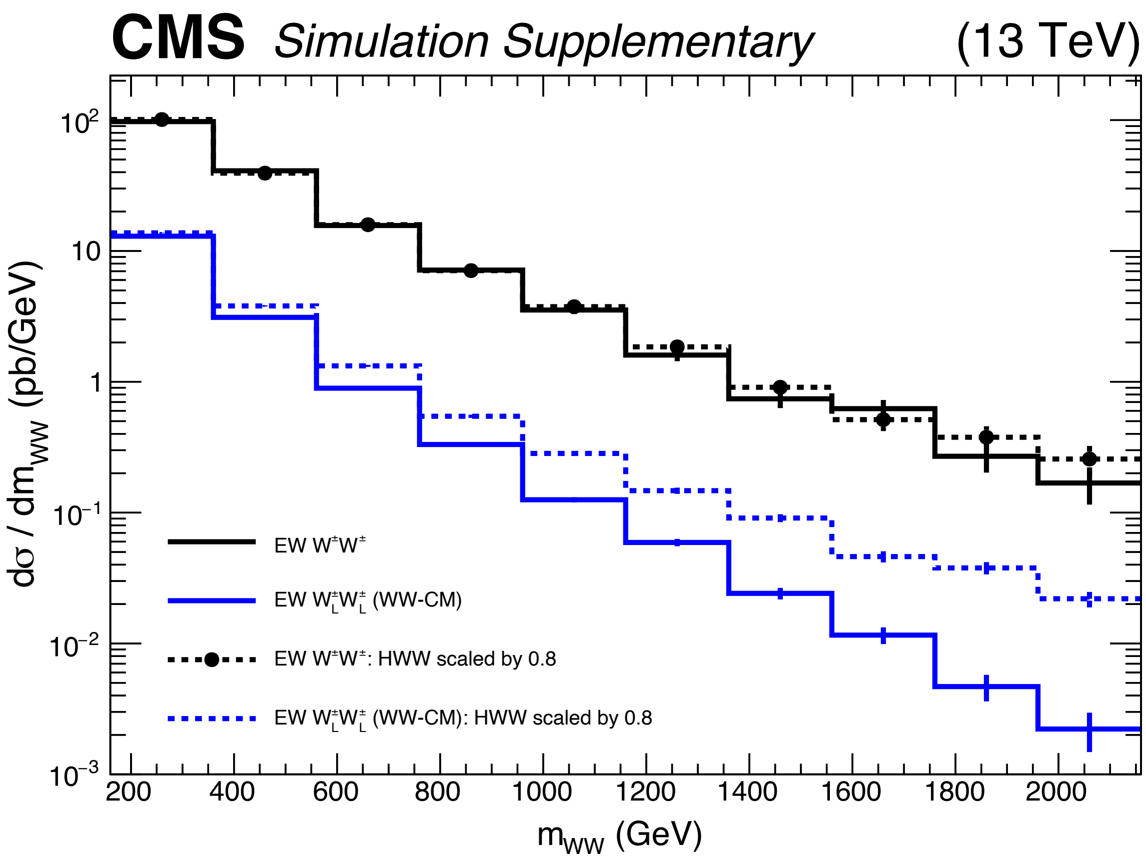

Longitudinal scattering and HL-LHC

- What about the longitudinal scattering?
  - Extremely challenging as the $W_L W_L \rightarrow W_L W_L$ is ~10% of the total WW scattering cross section
- High Luminosity LHC (HL-LHC) : the energy frontier for foreseeable future
  - CMS will collect ~3000fb^{-1}
  - Very bright lamp to see physics details->making it a challenging environment for the detectors and reconstruction

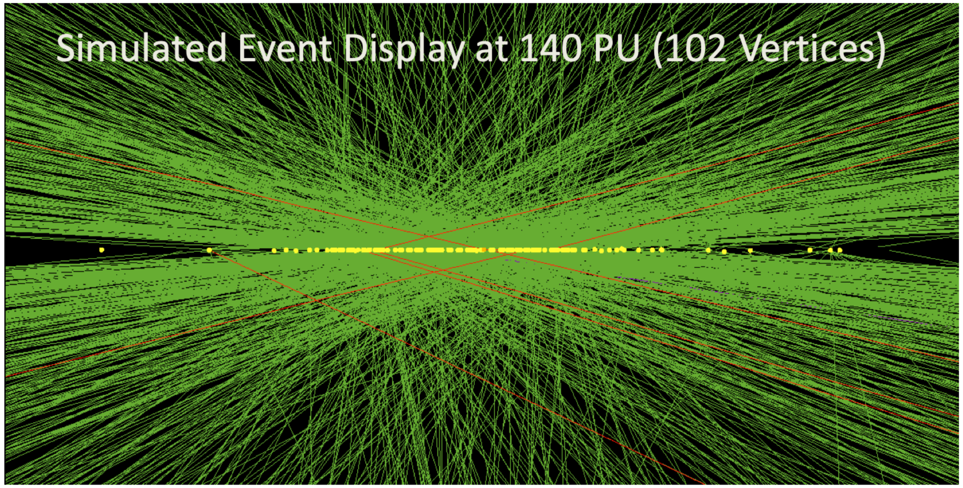

Polarized same-sign WW scattering

- First measurement of production cross sections for polarized same-sign WW scattering!
- Three distinct contributions: $W_L W_L$, $W_L W_T$, $W_T W_T$
    - Ideally we would measure all three components but the current data sample size is too limited
        - Measure $W_L W_L$ and $W_T W_X$ (X denotes either L or T)
        - Measure $W_L W_X$ and $W_T W_T$
- Polarization vectors are not Lorentz invariant and need to be defined for a given reference frame
    - Different polarization fractions and kinematic distributions
    - Two sets of results are reported with helicity eigenstates defined:
        - in WW center-of-mass reference frame
        - In parton-parton center of mass reference frame

Extracting polarization information

- Difficult to reconstruct the center-of-mass of each W boson due to presence of two neutrinos in the final state
  - Exploit kinematic differences with machine learning to separate the different polarized scattering processes
    - Separate BDTs are trained to separate $W_L W_L / W_T W_X$ and $W_L W_X / W_T W_T$ contributions for each reference frame

WW frame

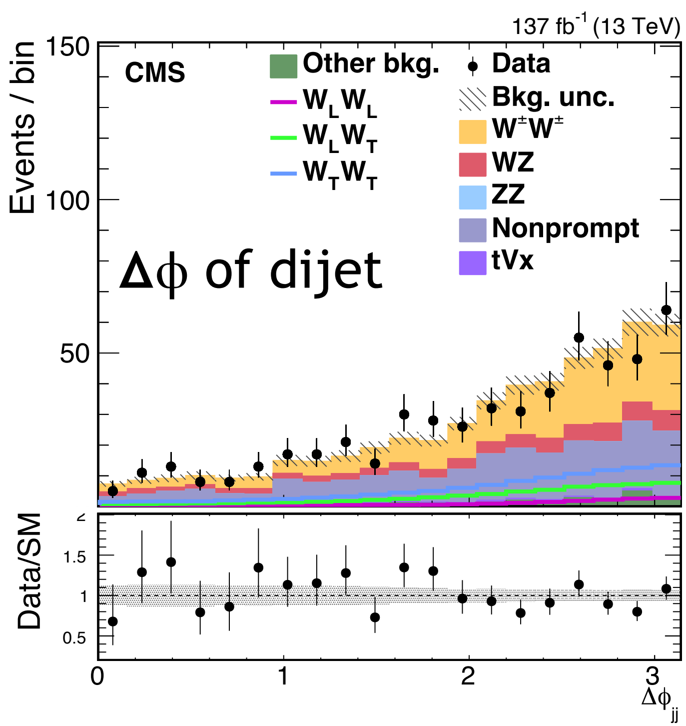

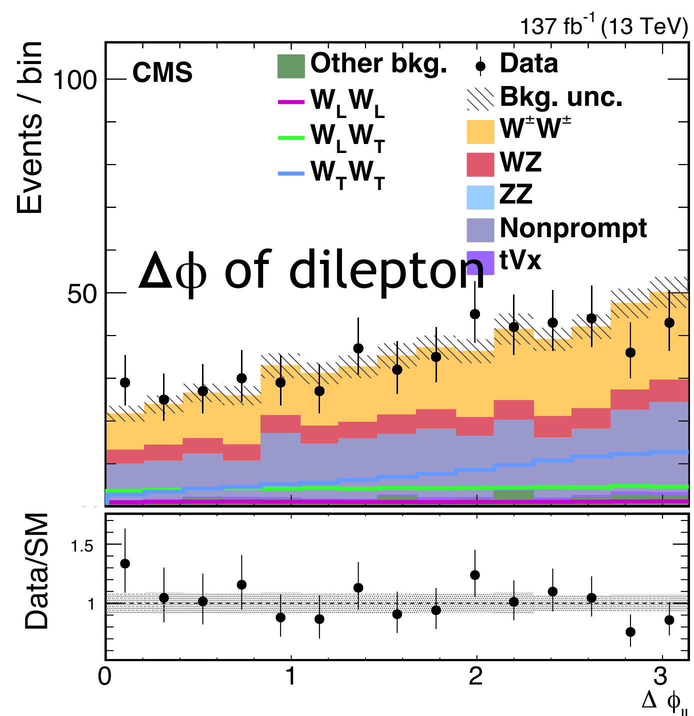

Extracting polarization information

Δϕ of dijet

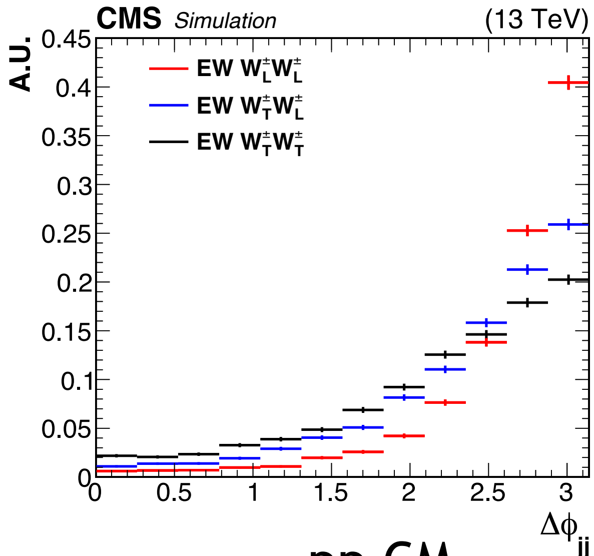

pp CM

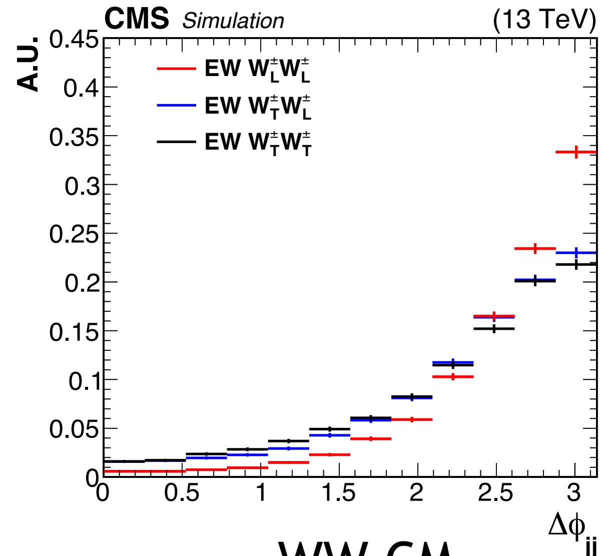

WW CM

Δϕ of dilepton

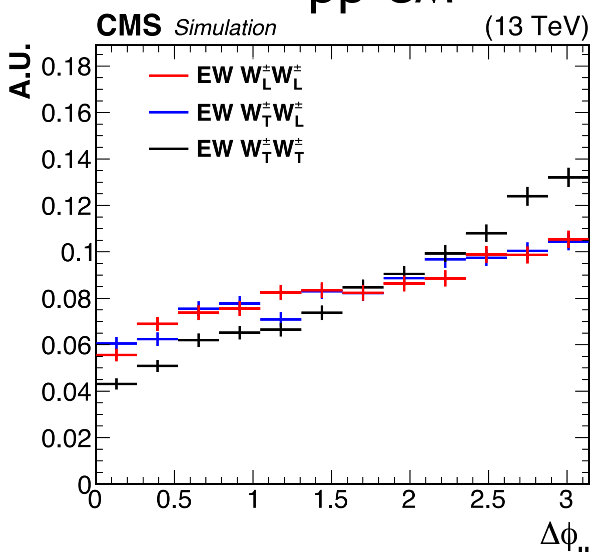

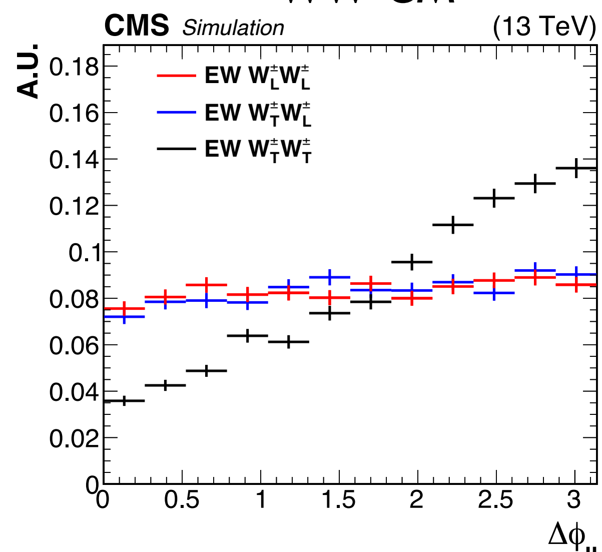

Signal BDT training

Variables	Definitions
$\Delta\phi_{jj}$	Difference in azimuthal angle between the leading and subleading jets
p_T^{j1}	p_T of the leading jet
p_T^{j2}	p_T of the subleading jet
$p_T^{\ell_1}$	Leading lepton p_T
$p_T^{\ell_2}$	Subleading lepton p_T
$\Delta\phi_{\ell\ell}$	Difference in azimuthal angle between the two leptons
$m_{\ell\ell}$	Dilepton mass
$p_T^{\ell\ell}$	Dilepton p_T
m_T^{WW}	Transverse WW diboson mass
$z^*_{\ell_1}$	Zeppenfeld variable of the leading lepton
$z^*_{\ell_2}$	Zeppenfeld variable of the subleading lepton
$\Delta R_{j1,\ell\ell}$	ΔR between the leading jet and the dilepton system
$\Delta R_{j2,\ell\ell}$	ΔR between the subleading jet and the dilepton system
$(p_T^{\ell_1} p_T^{\ell_2})/(p_T^{j1} p_T^{j2})$	Ratio of p_T products between leptons and jets
p_T^{miss}	Missing transverse momentum

Analysis strategy

- Analysis strategy: simultaneous fit in the $W^{\pm}W^{\pm}$ signal region and control regions to measure normalization of main background processes in situ
  - Train inclusive BDT to separate EW $W^{\pm}W^{\pm}$ production from SM backgrounds
  - Use 2-dimensional distribution of signal and inclusive BDT for the cross section fit in the signal region

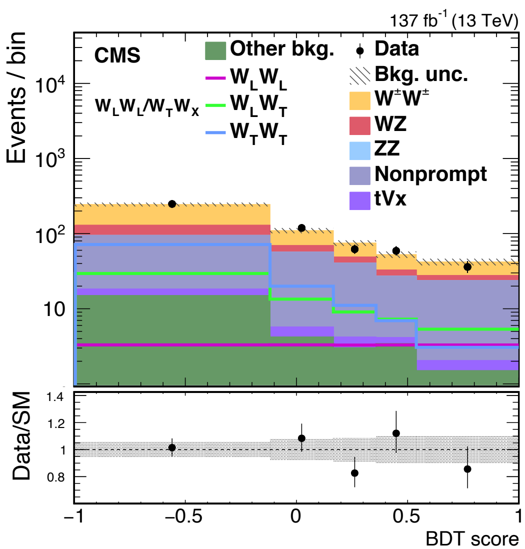

W_LW_L/W_TW_X

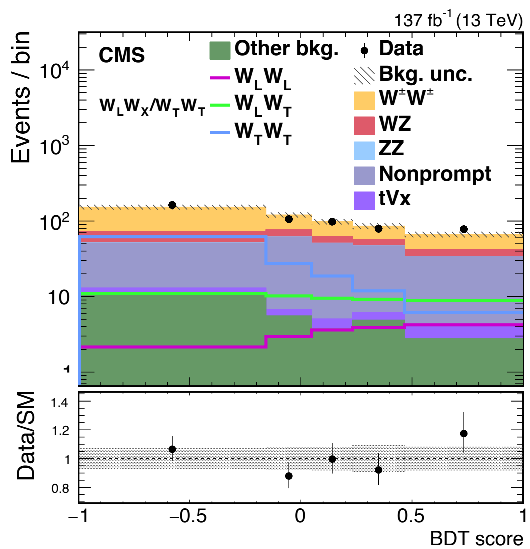

W_LW_X/W_TW_T

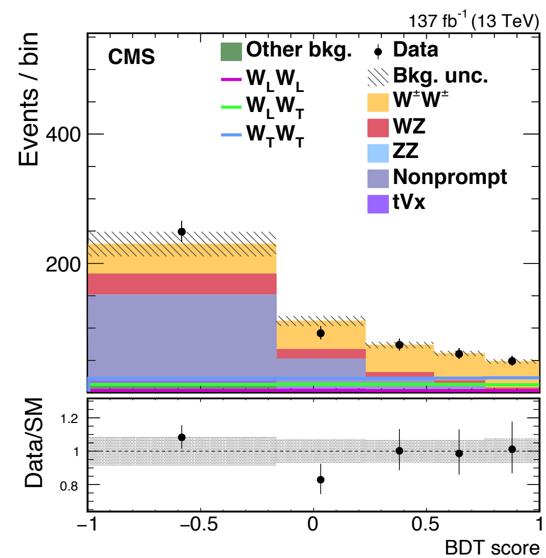

Inclusive BDT

Results

- First measurement of polarized VBS
    - Results are consistent with SM predictions
- Observed (expected) significance of 2.3 (3.1) standard deviations for $W_L W_X$ production
    - 2.6 (2.9) standard deviations in parton–parton frame
- Observed (expected) 95% CL upper limit of 1.17 (0.88) fb for $W_L W_L$ production (~2xSM prediction)
    - 1.06 (0.85) in parton–parton frame

Process	$\sigma\mathcal{B}$ (fb)	Theoretical prediction (fb)
$W^{\pm}_{L}W^{\pm}_{L}$	$0.32^{+0.42}_{-0.40}$	0.44 ± 0.05
$W^{\pm}_{X}W^{\pm}_{T}$	$3.06^{+0.51}_{-0.48}$	3.13 ± 0.35
$W^{\pm}_{L}W^{\pm}_{X}$	$1.20^{+0.56}_{-0.53}$	1.63 ± 0.18
$W^{\pm}_{T}W^{\pm}_{T}$	$2.11^{+0.49}_{-0.47}$	1.94 ± 0.21

WW frame

Process	$\sigma\mathcal{B}$ (fb)	Theoretical prediction (fb)
$W^{\pm}_{L}W^{\pm}_{L}$	$0.24^{+0.40}_{-0.37}$	0.28 ± 0.03
$W^{\pm}_{X}W^{\pm}_{T}$	$3.25^{+0.50}_{-0.48}$	3.32 ± 0.37
$W^{\pm}_{L}W^{\pm}_{X}$	$1.40^{+0.60}_{-0.57}$	1.71 ± 0.19
$W^{\pm}_{T}W^{\pm}_{T}$	$2.03^{+0.51}_{-0.50}$	1.89 ± 0.21

Parton-parton frame

Going beyond SM

- Hints of new physics using effective field theory approach to probe for anomalous TGC and QGC

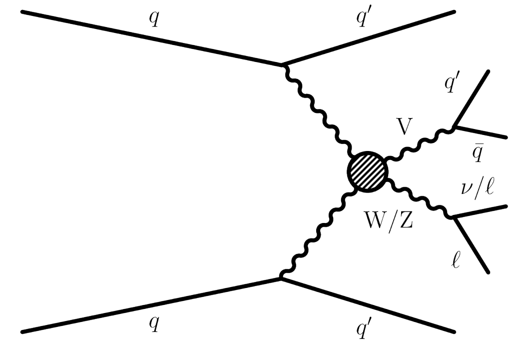

$$\mathcal{L} = \mathcal{L}_{\rm SM} + \sum_i \frac{c_i}{\Lambda^2}\mathcal{O}^i_{\rm dim-6} + \sum_j \frac{c_j}{\Lambda^4}\mathcal{O}^j_{\rm dim-8} + \ldots$$

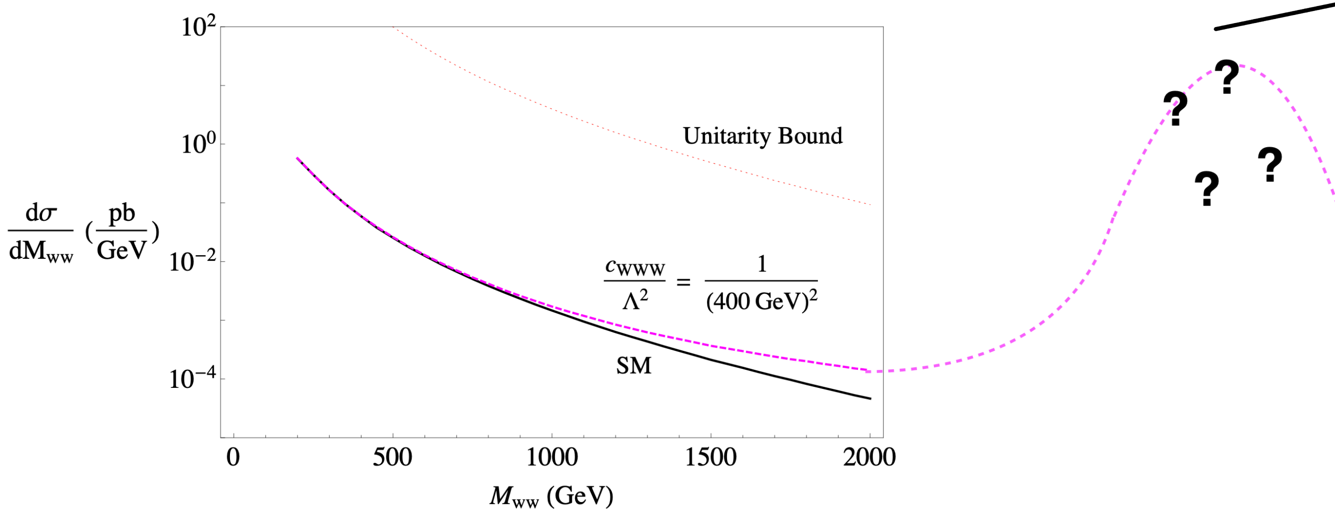

C. Degrande et al arxiv:1205.4231

Historic example: 4-fermion vertex (dim-6), Weak Interactions

$\Lambda = M_W$  $\xrightarrow{q^2 << M_W^2}$  $\propto \frac{g^2}{8}\frac{1}{M_W^2} = \frac{G_F}{\sqrt{2}}$

$\propto \frac{g^2}{8}\frac{1}{q^2 - M_W^2}$

Limits on dim-8 operators

- aQGC basis from Eboli et al (hep-ph/0606118)

$$\mathcal{O}_{S_0} = \left[(D_\mu \Phi)^\dagger D_\nu \Phi \right] \times \left[(D^\mu \Phi)^\dagger D^\nu \Phi \right]$$
$$\mathcal{O}_{S_1} = \left[(D_\mu \Phi)^\dagger D^\mu \Phi \right] \times \left[(D_\nu \Phi)^\dagger D^\nu \Phi \right]$$
$$\mathcal{O}_{S_2} = \left[(D_\mu \Phi)^\dagger D_\nu \Phi \right] \times \left[(D^\nu \Phi)^\dagger D^\mu \Phi \right]$$

$$\mathcal{O}_{M_0} = \mathrm{Tr}\left[W_{\mu\nu} W^{\mu\nu} \right] \times \left[(D_\beta \Phi)^\dagger D^\beta \Phi \right],$$
$$\mathcal{O}_{M_1} = \mathrm{Tr}\left[W_{\mu\nu} W^{\nu\beta} \right] \times \left[(D_\beta \Phi)^\dagger D^\mu \Phi \right],$$
$$\mathcal{O}_{M_2} = \left[B_{\mu\nu} B^{\mu\nu} \right] \times \left[(D_\beta \Phi)^\dagger D^\beta \Phi \right],$$
$$\mathcal{O}_{M_3} = \left[B_{\mu\nu} B^{\nu\beta} \right] \times \left[(D_\beta \Phi)^\dagger D^\mu \Phi \right],$$
$$\mathcal{O}_{M_4} = \left[(D_\mu \Phi)^\dagger W_{\beta\nu} D^\mu \Phi \right] \times B^{\beta\nu},$$
$$\mathcal{O}_{M_5} = \left[(D_\mu \Phi)^\dagger W_{\beta\nu} D^\nu \Phi \right] \times B^{\beta\mu},$$
$$\mathcal{O}_{M_7} = \left[(D_\mu \Phi)^\dagger W_{\beta\nu} W^{\beta\mu} D^\nu \Phi \right].$$

- Nominally no consideration is given for tree level unitarity violations
  - Same-sign WW and WZ bounds also reported with “Clipping” technique (cutting off EFT expansion at unitarity limit)

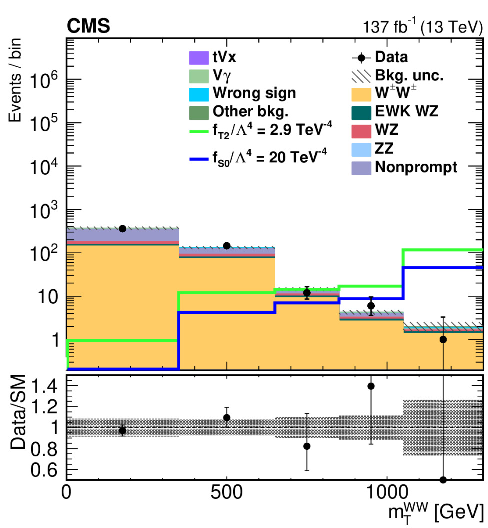

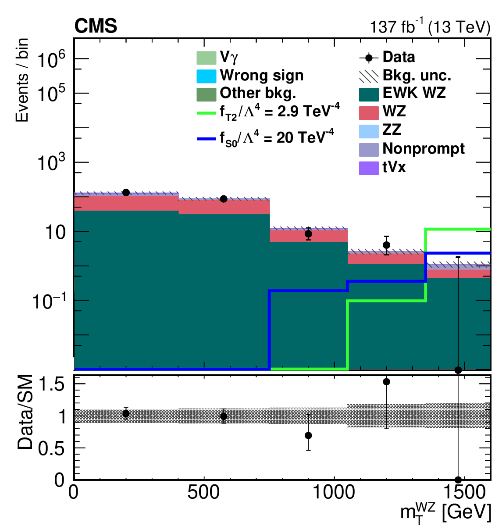

Limits on dim-8 operators

W$^{\pm}$W$^{\pm}$ & WZ without considering unitarity bounds

	Observed (W$^{\pm}$W$^{\pm}$) (TeV^{-4})	Expected (W$^{\pm}$W$^{\pm}$) (TeV^{-4})	Observed (WZ) (TeV^{-4})	Expected (WZ) (TeV^{-4})	Observed (TeV^{-4})	Expected (TeV^{-4})
f_{T0}/Λ^4	[-0.28, 0.31]	[-0.36, 0.39]	[-0.62, 0.65]	[-0.82, 0.85]	[-0.25, 0.28]	[-0.35, 0.37]
f_{T1}/Λ^4	[-0.12, 0.15]	[-0.16, 0.19]	[-0.37, 0.41]	[-0.49, 0.55]	[-0.12, 0.14]	[-0.16, 0.19]
f_{T2}/Λ^4	[-0.38, 0.50]	[-0.50, 0.63]	[-1.0 , 1.3]	[-1.4, 1.7]	[-0.35, 0.48]	[-0.49, 0.63]
f_{M0}/Λ^4	[-3.0, 3.2]	[-3.7, 3.8]	[-5.8, 5.8]	[-7.6, 7.6]	[-2.7, 2.9]	[-3.6, 3.7]
f_{M1}/Λ^4	[-4.7, 4.7]	[-5.4, 5.8]	[-8.2, 8.3]	[-11, 11]	[-4.1, 4.2]	[-5.2, 5.5]
f_{M6}/Λ^4	[-6.0, 6.5]	[-7.5, 7.6]	[-12, 12]	[-15, 15]	[-5.4, 5.8]	[-7.2, 7.3]
f_{M7}/Λ^4	[-6.7, 7.0]	[-8.3, 8.1]	[-10, 10]	[-14, 14]	[-5.7, 6.0]	[-7.8, 7.6]
f_{S0}/Λ^4	[-6.0, 6.4]	[-6.0, 6.2]	[-19, 19]	[-24, 24]	[-5.7, 6.1]	[-5.9, 6.2]
f_{S1}/Λ^4	[-18, 19]	[-18, 19]	[-30, 30]	[-38, 39]	[-16, 17]	[-18, 18]

W$^{\pm}$W$^{\pm}$ & WZ considering unitarity bounds

	Observed (W$^{\pm}$W$^{\pm}$) (TeV^{-4})	Expected (W$^{\pm}$W$^{\pm}$) (TeV^{-4})	Observed (WZ) (TeV^{-4})	Expected (WZ) (TeV^{-4})	Observed (TeV^{-4})	Expected (TeV^{-4})
f_{T0}/Λ^4	[-1.5, 2.3]	[-2.1, 2.7]	[-1.6, 1.9]	[-2.0, 2.2]	[-1.1, 1.6]	[-1.6, 2.0]
f_{T1}/Λ^4	[-0.81, 1.2]	[-0.98, 1.4]	[-1.3, 1.5]	[-1.6, 1.8]	[-0.69, 0.97]	[-0.94, 1.3]
f_{T2}/Λ^4	[-2.1, 4.4]	[-2.7, 5.3]	[-2.7, 3.4]	[-4.4, 5.5]	[-1.6, 3.1]	[-2.3, 3.8]
f_{M0}/Λ^4	[-13, 16]	[-19, 18]	[-16, 16]	[-19, 19]	[-11, 12]	[-15, 15]
f_{M1}/Λ^4	[-20, 19]	[-22, 25]	[-19, 20]	[-23, 24]	[-15, 14]	[-18, 20]
f_{M6}/Λ^4	[-27, 32]	[-37, 37]	[-34, 33]	[-39, 39]	[-22, 25]	[-31, 30]
f_{M7}/Λ^4	[-22, 24]	[-27, 25]	[-22, 22]	[-28, 28]	[-16, 18]	[-22, 21]
f_{S0}/Λ^4	[-35, 36]	[-31, 31]	[-83, 85]	[-88, 91]	[-34, 35]	[-31, 31]
f_{S1}/Λ^4	[-100, 120]	[-100, 110]	[-110, 110]	[-120, 130]	[-86, 99]	[-91, 97]

Semileptonic final states

- Semileptonic WV process where one boson decays to quarks
- W±Vjj includes contributions from:
  - W±W±jj, W±Wjj, and W±Zjj VBS processes

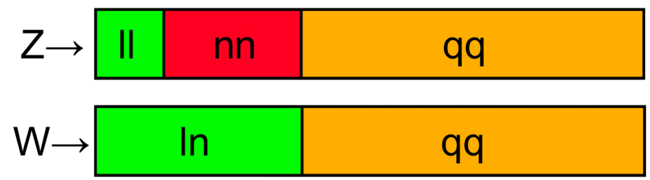

- W/Z in VBS events can be highly boosted
- V-jet tagging via substructure techniques

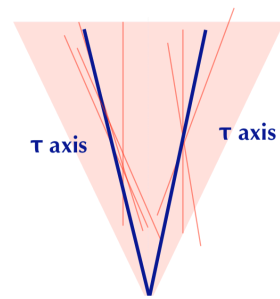

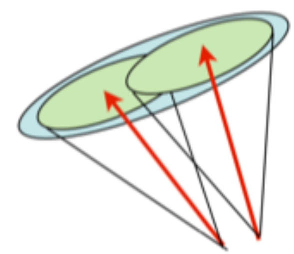

ArXiv:1905.07445

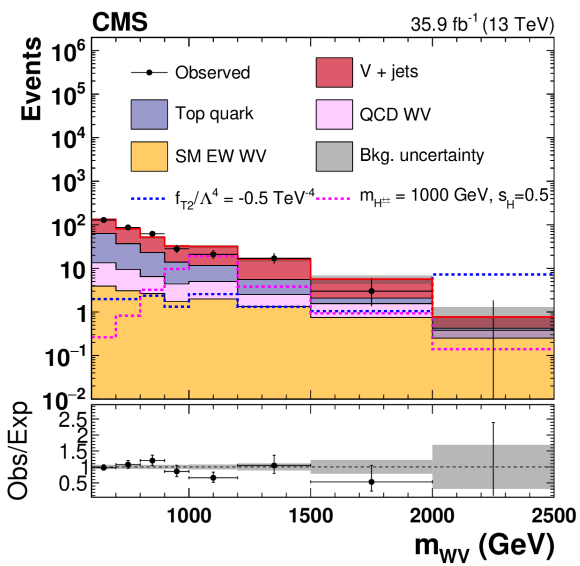

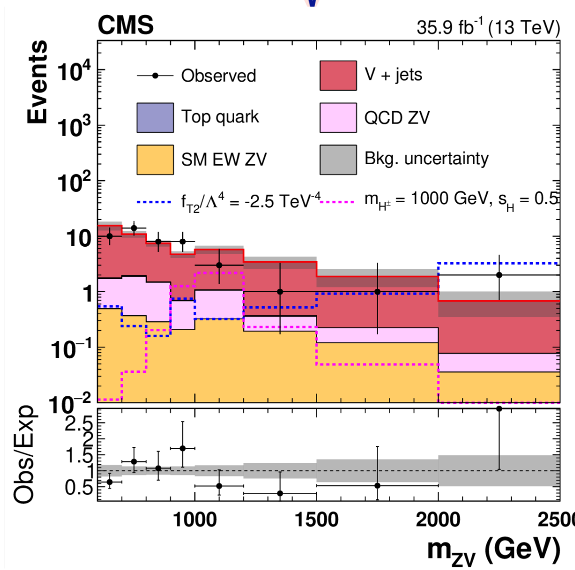

Limits on dim-8 operators

- Semileptonic final state provides the most stringent limits on this parameters to date (using the 2016 dataset 35.9 fb^{-1})

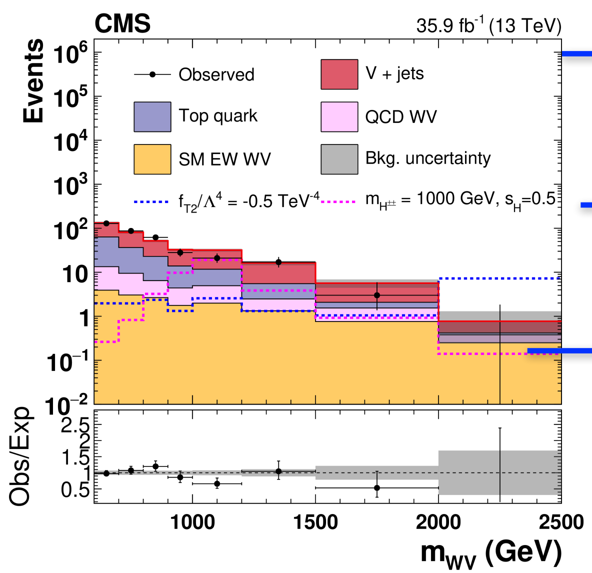

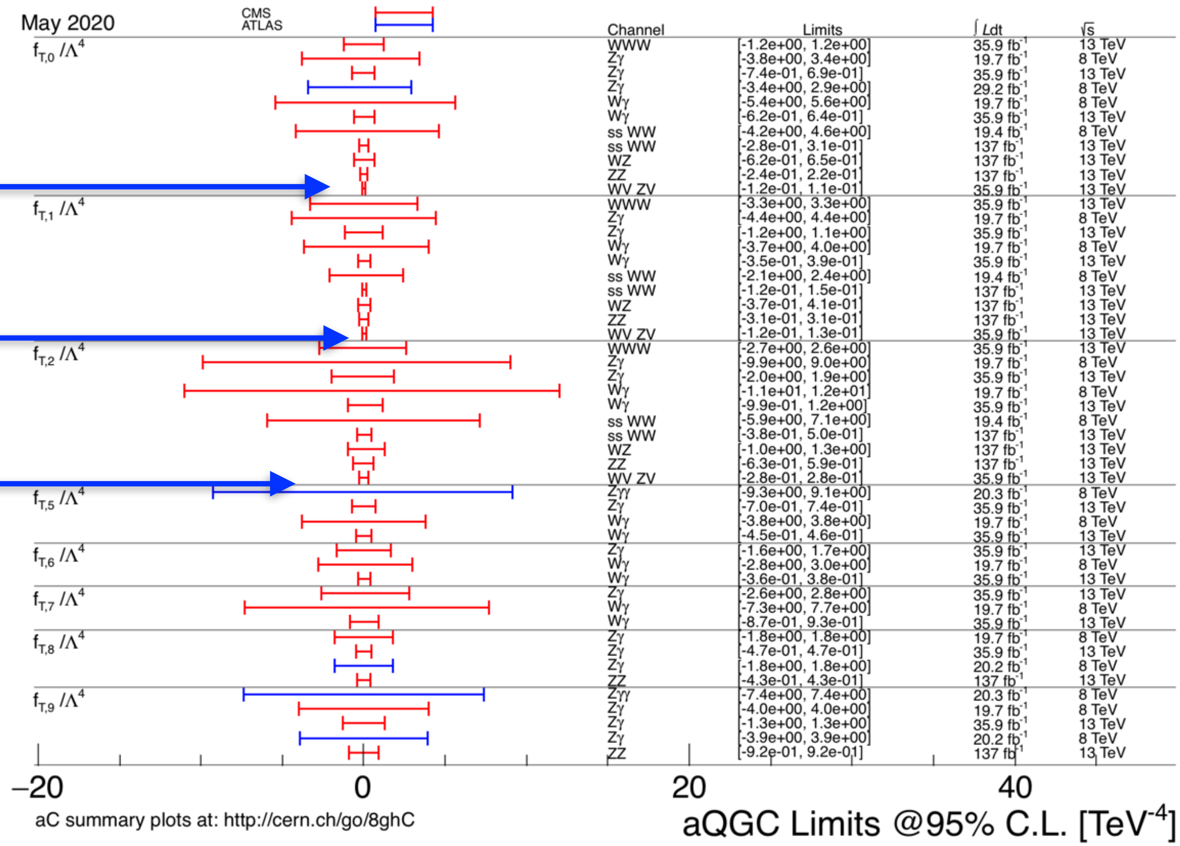

Extended Higgs sector

- Two-Higgs-double model (2HDM) - Minimal extension of SM
  - Five physical scalar states: h, H, A, H^+, H^-
- Higgs triplet extensions
  - Georgi-Machacek: One real and one complex triplet
  - Tree level H^+ WZ coupling
  - Presence of doubly charged higgs: H^{++}

$$\Phi = \begin{pmatrix} \phi_2^* & \phi_1 \\ -\phi_1^* & \phi_2 \end{pmatrix}, \qquad \Xi = \begin{pmatrix} \chi_3^* & \xi_1 & \chi_1 \\ -\chi_2^* & \xi_2 & \chi_2 \\ \chi_1^* & -\xi_1^* & \chi_3 \end{pmatrix}.$$

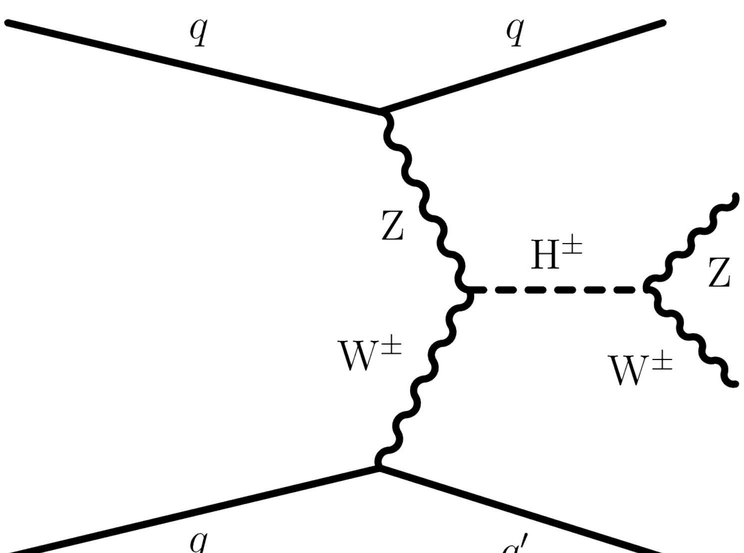

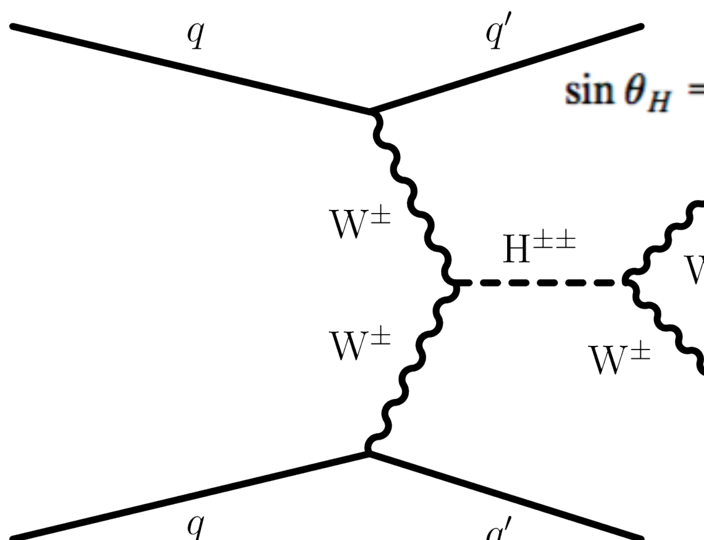

$$\sin\theta_H =: s_H = \frac{2\sqrt{2}v_\Xi}{v_{\mathrm{SM}}}$$

Extended Higgs sector

- Extend to much higher mass regime compared to Run 1

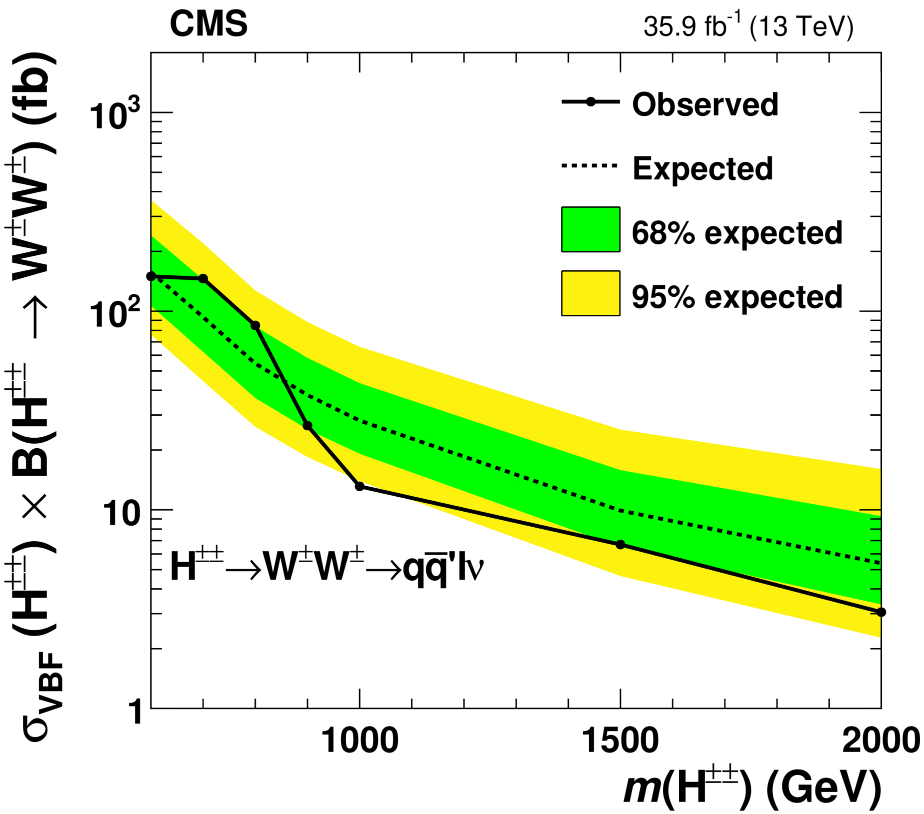

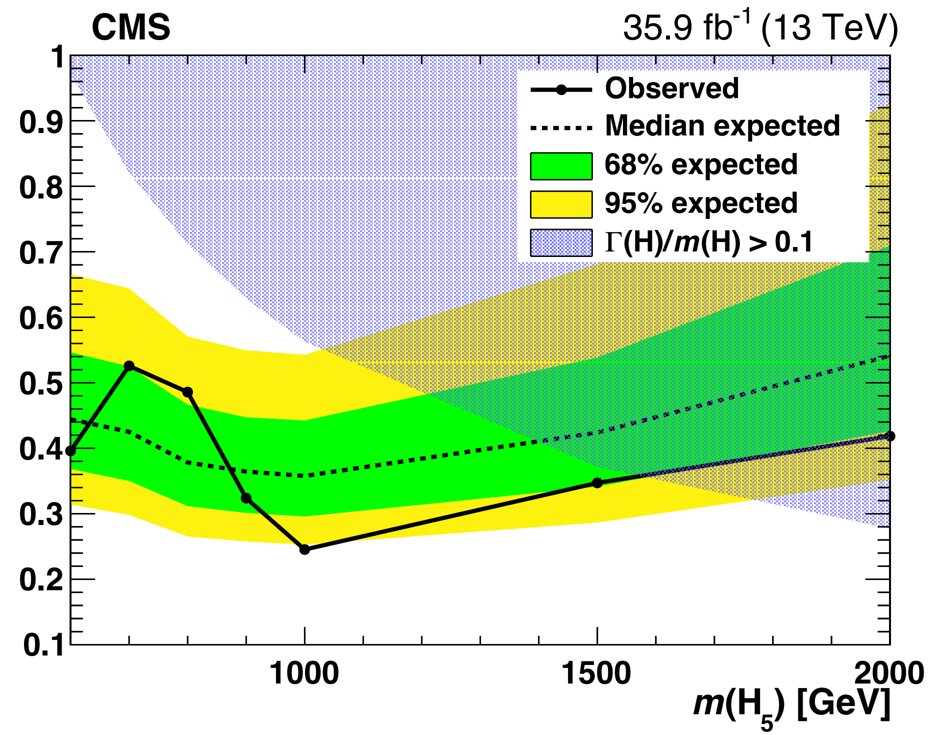

Summary of CMS EW measurements

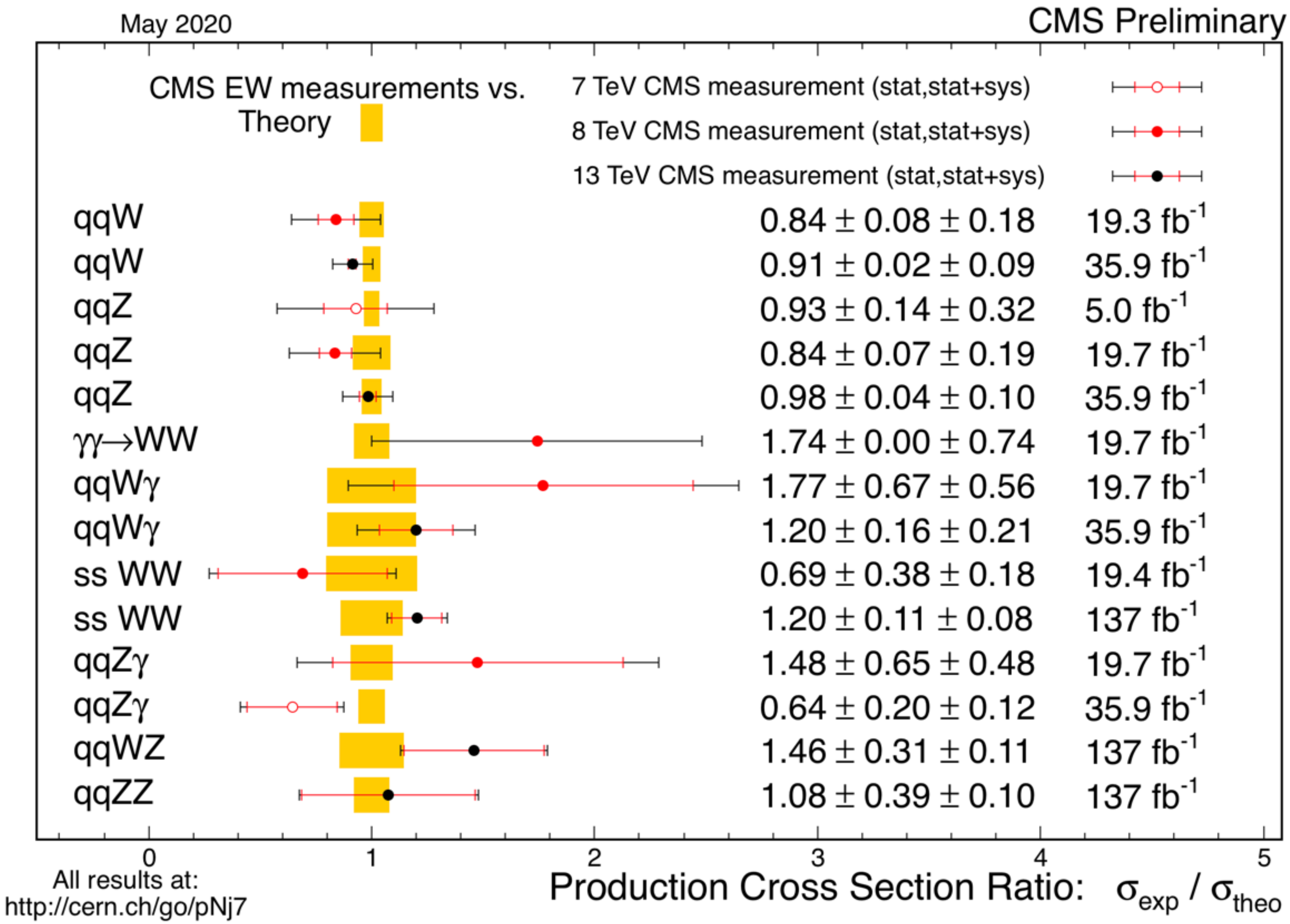

Summary

- Consistency tests of the EW sector of SM at the LHC
    - No significant deviations so far
- VBS measurements probing non-abelian gauge structure of the SM
    - Key measurements to fully explore EW symmetry breaking
    - From first observations of rare EW processes to precision measurements -> strong constraints on New Physics
- (HL-) LHC datasets are growing
    - ~1% analyzed so far
    - ~4% recorded and partly analyzed

- Extensive work, challenges and opportunities ahead to collect quality data and produce quality physics

ADDITIONAL MATERIAL

Distributions in WW signal region

Good agreement between data and prediction

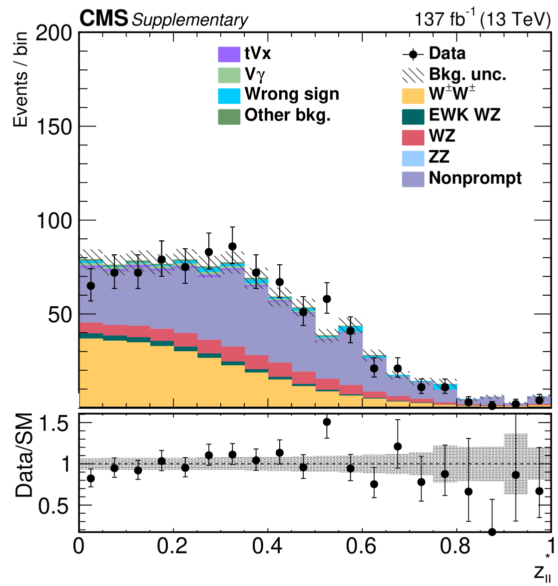

Zeppenfeld variable

$$z^*_\ell = \left|\eta^\ell - \frac{\eta^{j_1} + \eta^{j_2}}{2}\right| / |\Delta\eta_{jj}|$$

Phys. Rev. D 54 (1996) 6680

Number of jets with p_T>30 GeV

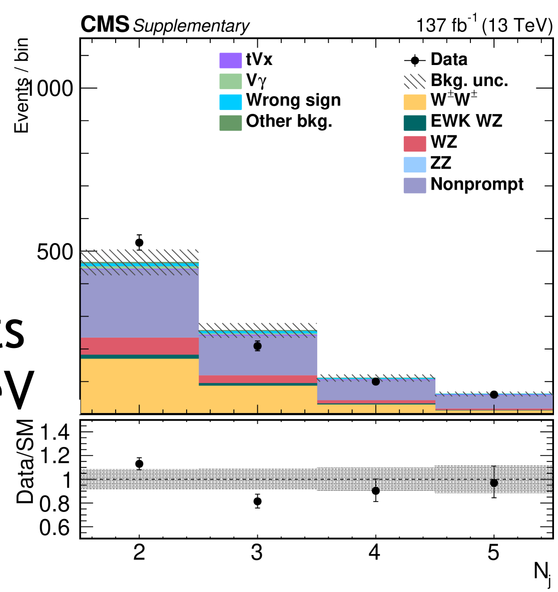

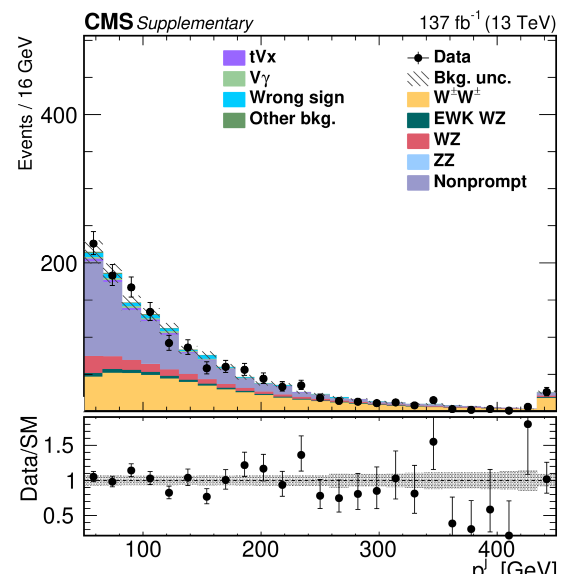

p_T of jets

Distributions in WZ signal region

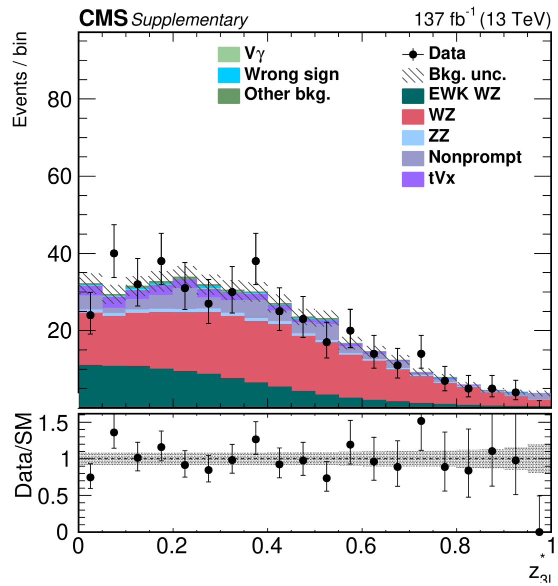

Good agreement between data and prediction

Zeppenfeld variable

$$z^*_\ell = \left|\eta^\ell - \frac{\eta^{j_1} + \eta^{j_2}}{2}\right| / |\Delta\eta_{jj}|$$

Phys. Rev. D 54 (1996) 6680

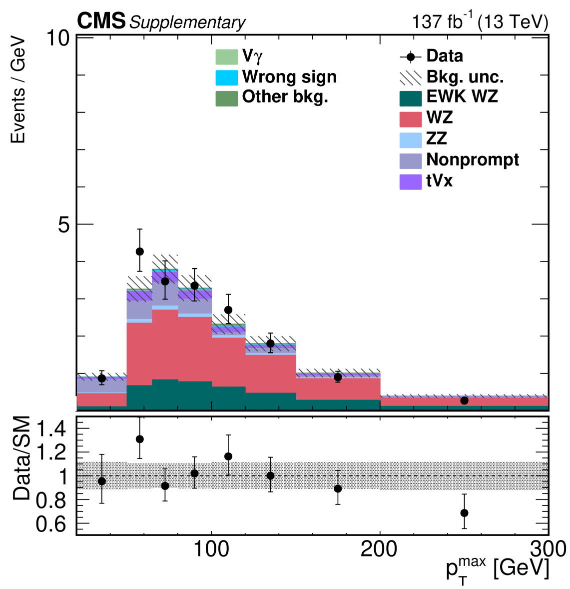

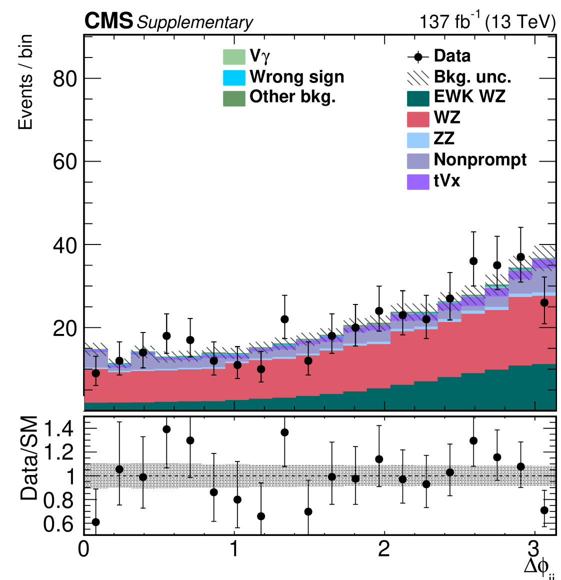

Leading lepton p_T

$\Delta\phi$ of the two jets

Event selection

Variable	$W^{\pm}W^{\pm}$	WZ
Leptons	2ℓ, $p_T > 25/20\text{GeV}$	3ℓ, $p_T > 25/10/20\text{GeV}$
p_T^j	$>50\text{GeV}$	$>50\text{GeV}$
$\lvert m_{\ell\ell} - m_Z \rvert$	$>15\text{GeV(ee)}$	$<15\text{GeV}$
$m_{\ell\ell}$	$>20\text{GeV}$	–
$m_{\ell\ell\ell}$	–	$>100\text{GeV}$
p_T^{miss}	$>30\text{GeV}$	$>30\text{GeV}$
b quark veto	Required	Required
$\max(z_\ell^*)$	<0.75	<1.0
m_{jj}	$>500\text{GeV}$	$>500\text{GeV}$
$\lvert\Delta\eta_{jj}\rvert$	>2.5	>2.5

$$z_\ell^* = \left|\eta^\ell - \frac{\eta^{j_1} + \eta^{j_2}}{2}\right| / |\Delta\eta_{jj}|$$

Tight lepton selection to reduce nonprompt lepton background

Only electrons and muons are considered

Yields

Table 4: Expected yields from SM processes and observed data events in $W^\pm W^\pm$ and WZ SRs. The combination of the statistical and systematic uncertainties is shown. The expected yields are shown with their best fit normalizations from the simultaneous fit to the Asimov data set and to the data. The signal yields do not include the QCD and EW NLO corrections.

Process	$W^\pm W^\pm$ SR		WZ SR	
	Asimov data set	Data	Asimov data set	Data
EW $W^\pm W^\pm$	209 ± 26	210 ± 26	—	—
QCD $W^\pm W^\pm$	13.8 ± 1.6	13.7 ± 2.2	—	—
Interference $W^\pm W^\pm$	8.4 ± 2.3	8.7 ± 2.3	—	—
EW WZ	14.1 ± 4.0	17.8 ± 3.9	54 ± 15	69 ± 15
QCD WZ	43 ± 6.7	42.7 ± 7.4	118 ± 17	117 ± 17
Interference WZ	0.3 ± 0.1	0.3 ± 0.2	2.2 ± 0.9	2.7 ± 1.0
ZZ	0.7 ± 0.2	0.7 ± 0.2	6.1 ± 1.7	6.0 ± 1.8
Nonprompt	211 ± 43	193 ± 40	14.6 ± 7.4	14.4 ± 6.7
tVx	7.8 ± 1.9	7.4 ± 2.2	15.1 ± 2.7	14.3 ± 2.8
$W\gamma$	9.0 ± 1.8	9.1 ± 2.9	1.1 ± 0.3	1.1 ± 0.4
Wrong-sign	13.5 ± 6.5	13.9 ± 6.5	1.6 ± 0.5	1.7 ± 0.7
Other background	5.0 ± 1.3	5.2 ± 2.1	3.3 ± 0.6	3.3 ± 0.7
Total SM	535 ± 52	522 ± 49	216 ± 21	229 ± 23
Data	524		229	

Boosted decision tree for EW WZ

- Enhance WZ EW production w.r.t large WZ QCD production
- 13 Input variables retained out of a larger set tested
- Improved sensitivity w.r.t. using m_{jj}–$|\Delta\eta_{\mathrm{jj}}|$ by $\sim$20%

Variable	Definition
m_{jj}	Mass of the leading and trailing jets system
$\|\Delta\eta_{\mathrm{jj}}\|$	Absolute difference in rapidity of the leading and trailing jets
$\Delta\phi_{\mathrm{jj}}$	Absolute difference in azimuthal angles of the leading and trailing jets
$p_{\mathrm{T}}^{\mathrm{j1}}$	p_{T} of the leading jet
$p_{\mathrm{T}}^{\mathrm{j2}}$	p_{T} of the trailing jet
η^{j1}	Pseudorapidity of the leading jet
$\|\eta^{\mathrm{W}} - \eta^{\mathrm{Z}}\|$	Absolute difference between η^{W} and η^{Z}
$z^{*}_{\ell_i} (i = 1 - 3)$	Zeppenfeld variable of the three selected leptons
$z^{*}_{3\ell}$	Zeppenfeld variable of the vector sum of the three leptons
$\Delta R_{\mathrm{j1,Z}}$	ΔR between the leading jet and the Z boson
$\|\vec{p_{\mathrm{T}}}^{\mathrm{tot}}\| / \sum_i p_{\mathrm{T}}^{i}$	Vector sum p_{T} normalized to their scalar p_{T} sum

Background estimation

- Combination of data-driven methods and detailed simulation studies to estimate backgrounds
  - nonprompt lepton background estimated from data, in addition to a CR
  - Charge-misidentification electron rate estimated using $\mathrm{Z} \rightarrow \mathrm{ee}$
  - ZZ background normalized with a CR
  - tZq background normalized with a CR
  - other small background processes from simulation
- Analysis strategy: single fit with the following regions
  - $\mathrm{W}^{\pm}\mathrm{W}^{\pm}$ SR
  - WZ SR
  - nonprompt lepton background CR (inverting b-tagging)
  - tZq CR (inverting b-tagging)
  - ZZ CR (4 leptons)

Inclusive BDT training

Variables	Definitions
m_{jj}	Dijet mass
$\lvert\Delta\eta_{\mathrm{jj}}\rvert$	Difference in pseudorapidity between the leading and trailing jets
$\Delta\phi_{\mathrm{jj}}$	Difference in azimuth angles between the leading and trailing jets
$p_{\mathrm{T}}^{\mathrm{j1}}$	p_{T} of the leading jet
$p_{\mathrm{T}}^{\mathrm{j2}}$	p_{T} of the trailing jet
$p_{\mathrm{T}}^{\ell_1}$	Leading lepton p_{T}
$p_{\mathrm{T}}^{\mathrm{miss}}$	Missing transverse momentum
$p_{\mathrm{T}}^{\ell\ell}$	Dilepton p_{T}
$z^*_{\ell_1}$	Zeppenfeld variable of the leading lepton
$z^*_{\ell_2}$	Zeppenfeld variable of the trailing lepton

Detailed ZZjj selection

Object	Selection
	ZZjj inclusive
Leptons	$p_{\mathrm{T}}(\ell_1) > 20$ GeV
	$p_{\mathrm{T}}(\ell_2) > 10$ GeV
	$p_{\mathrm{T}}(\ell) > 5$ GeV
	$\lvert\eta(\ell)\rvert < 2.5$
	(γ with $\Delta R(\ell,\gamma) < 0.1$ added to ℓ 4-vector)
Z and ZZ	$60 < m(\ell\ell) < 120$ GeV
	$m(4\ell) > 180$ GeV
Jets	at least 2
	$p_{\mathrm{T}}(j) > 30$ GeV
	$\lvert\eta(j)\rvert < 4.7$
	$m_{jj} > 100$ GeV
	$\Delta R(\ell, j) > 0.4$ for each ℓ, j
	VBS-enriched (loose)
	ZZjj inclusive +
Jets	$\lvert\Delta\eta(jj)\rvert > 2.4$
	$m_{jj} > 400$ GeV
	VBS-enriched (tight)
	ZZjj inclusive +
Jets	$\lvert\Delta\eta(jj)\rvert > 5$
	$m_{jj} > 400$ GeV

Yields and cross section measurements

Year	Signal (ZZjj EW)	Z+X	$q\bar{q} \to$ ZZjj QCD	$gg \to$ ZZjj QCD	$t\bar{t}$ +VVZ	Total predicted	Data
			ZZjj inclusive				
2016	6.3 ± 0.7	2.8 ± 1.1	65.6 ± 9.5	13.5 ± 2.0	8.4 ± 2.2	97 ± 13	95
2017	7.4 ± 0.8	2.4 ± 0.9	77.7 ± 11.2	20.3 ± 3.0	9.6 ± 2.5	117 ± 15	121
2018	10.4 ± 1.1	4.1 ± 1.6	98.1 ± 14.2	29.1 ± 4.3	14.2 ± 3.8	156 ± 20	159
all	24.1 ± 2.5	9.4 ± 3.6	241.5 ± 34.9	62.9 ± 9.3	32.2 ± 8.5	370 ± 48	375
			VBS signal-enriched (loose)				
2016	4.2 ± 0.4	0.4 ± 0.2	9.7 ± 1.4	3.2 ± 0.5	1.1 ± 0.3	18.7 ± 2.3	21
2017	4.9 ± 0.5	0.5 ± 0.2	13.5 ± 1.9	5.5 ± 0.8	1.2 ± 0.3	25.5 ± 3.1	17
2018	6.9 ± 0.7	0.8 ± 0.3	14.9 ± 2.2	8.3 ± 1.2	1.7 ± 0.5	32.6 ± 3.9	30
all	16.0 ± 1.7	1.6 ± 0.6	38.1 ± 5.5	17.0 ± 2.5	4.1 ± 1.1	76.8 ± 9.3	68
			VBS signal-enriched (tight)				
2016	1.1 ± 0.1	0.05 ± 0.02	1.9 ± 0.3	1.0 ± 0.1	0.13 ± 0.03	4.2 ± 0.5	4
2017	1.2 ± 0.1	0.05 ± 0.02	3.6 ± 0.5	1.8 ± 0.3	0.13 ± 0.03	6.7 ± 0.8	2
2018	1.7 ± 0.2	0.12 ± 0.04	2.6 ± 0.4	2.2 ± 0.3	0.19 ± 0.05	6.8 ± 0.8	11
all	3.9 ± 0.4	0.22 ± 0.08	8.1 ± 1.2	4.9 ± 0.7	0.45 ± 0.12	17.6 ± 2.1	17

	SM σ (fb)	Measured σ (fb)
	ZZjj inclusive	
EW	0.275 ± 0.021(theo)	$0.33\ ^{+0.11}_{-0.10}$ (stat) $^{+0.04}_{-0.03}$ (syst)
EW+QCD	5.35 ± 0.51(theo)	$5.29\ ^{+0.31}_{-0.30}$ (stat) ± 0.46 (syst)
	VBS-enriched (loose)	
EW	0.186 ± 0.015 (theo)	$0.200\ ^{+0.078}_{-0.067}$ (stat) $^{+0.023}_{-0.013}$ (syst)
EW+QCD	1.21 ± 0.09 (theo)	$1.00\ ^{+0.12}_{-0.11}$ (stat) $^{+0.06}_{-0.05}$ (syst)
	VBS-enriched (tight)	
EW	0.050 ± 0.005 (theo)	$0.06\ ^{+0.05}_{-0.04}$ (stat) ± 0.01 (syst)
EW+QCD	0.171 ± 0.012 (theo)	0.17 ± 0.04 (stat) ± 0.01 (syst)

Systematic uncertainties

WW frame

Source of uncertainty	$W_L^\pm W_L^\pm$ (%)	$W_X^\pm W_T^\pm$ (%)	$W_L^\pm W_X^\pm$ (%)	$W_T^\pm W_T^\pm$ (%)
Integrated luminosity	3.2	1.8	1.9	1.8
Lepton measurement	3.6	1.9	2.5	1.8
Jet energy scale and resolution	11	2.9	2.5	1.1
Pileup	0.9	0.1	1.0	0.3
btagging	1.1	1.2	1.4	1.1
Nonprompt rate	17	2.7	9.3	1.6
Trigger	1.9	1.1	1.6	0.9
Limited sample size	38	3.9	14	5.7
Theory	6.8	2.3	4.0	2.3
Total systematic uncertainty	44	6.6	18	7.0
Statistical uncertainty	123	15	42	22
Total uncertainty	130	16	46	23

Extracting polarization information

Dilepton mass

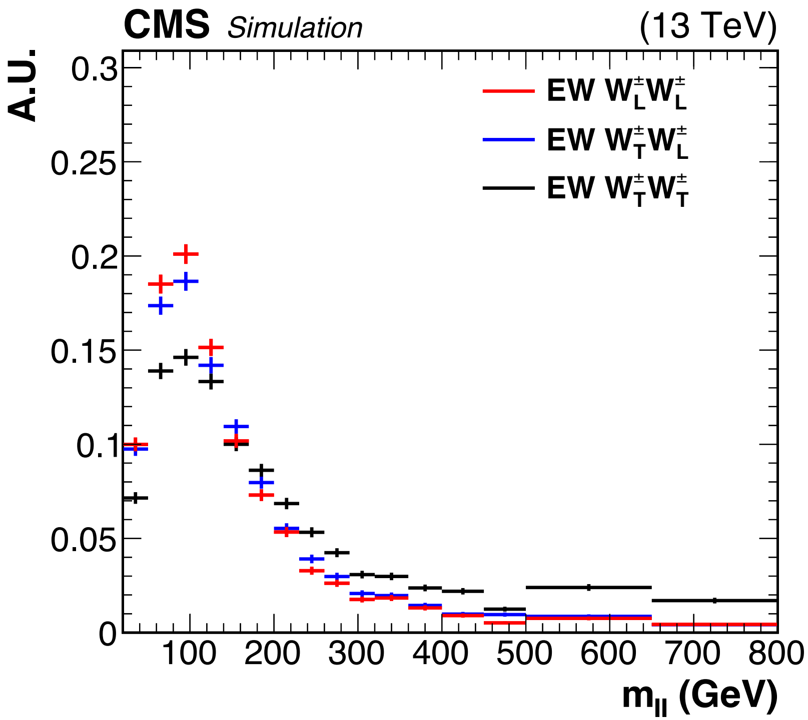

pp CM

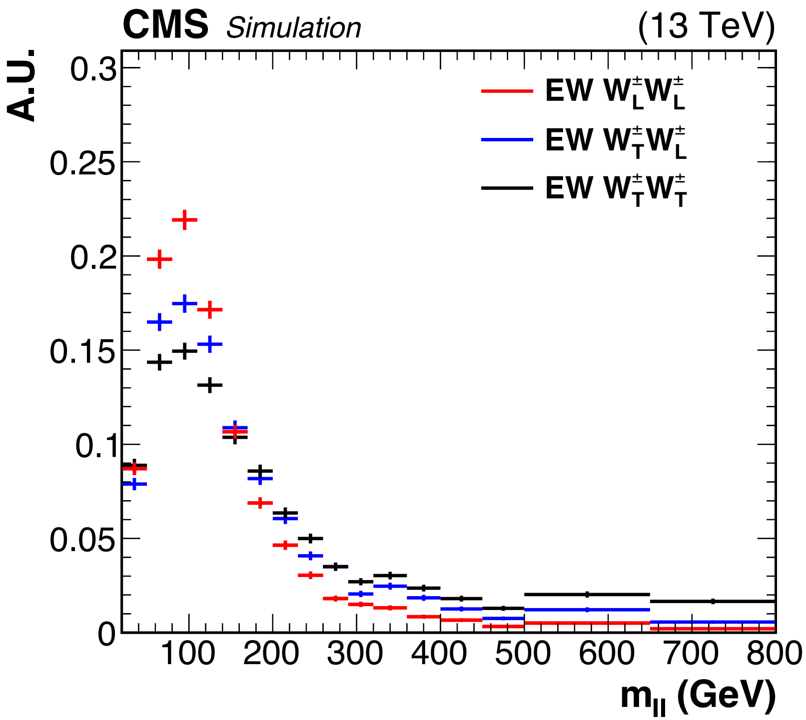

WW CM

Polarized WW samples

Δϕ of dijet

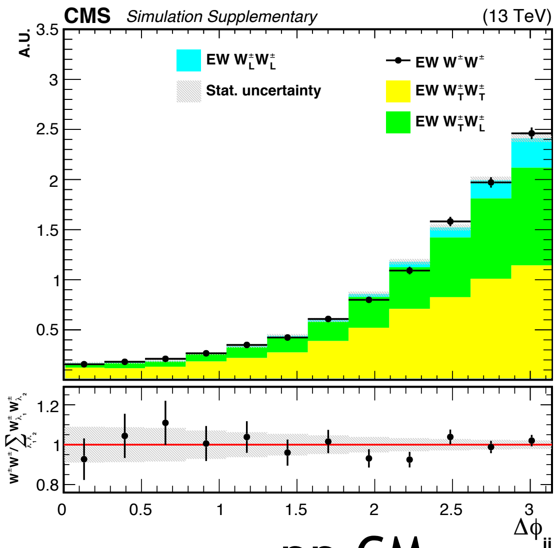

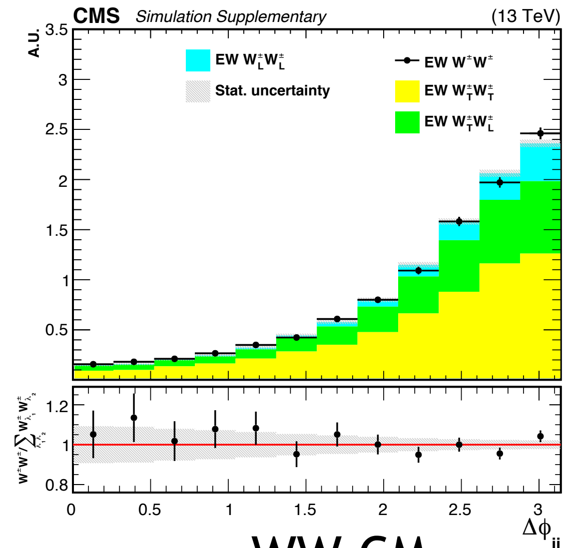

pp CM

WW CM

Δϕ of dilepton

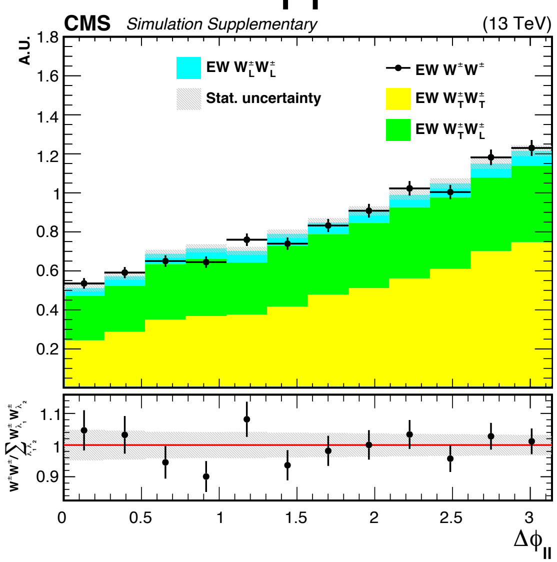

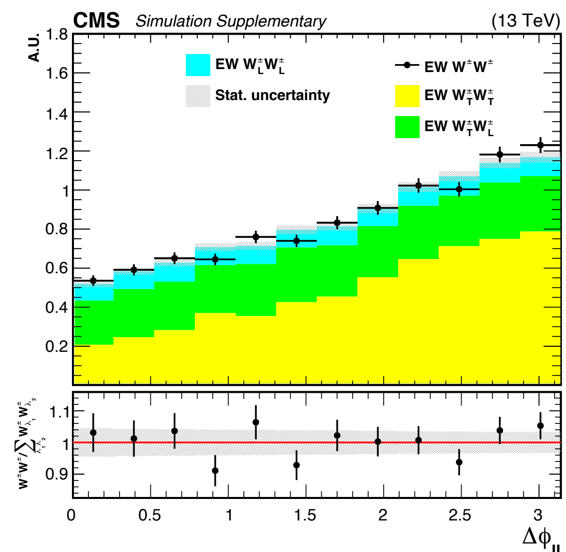

Polarized WW samples

Dilepton mass

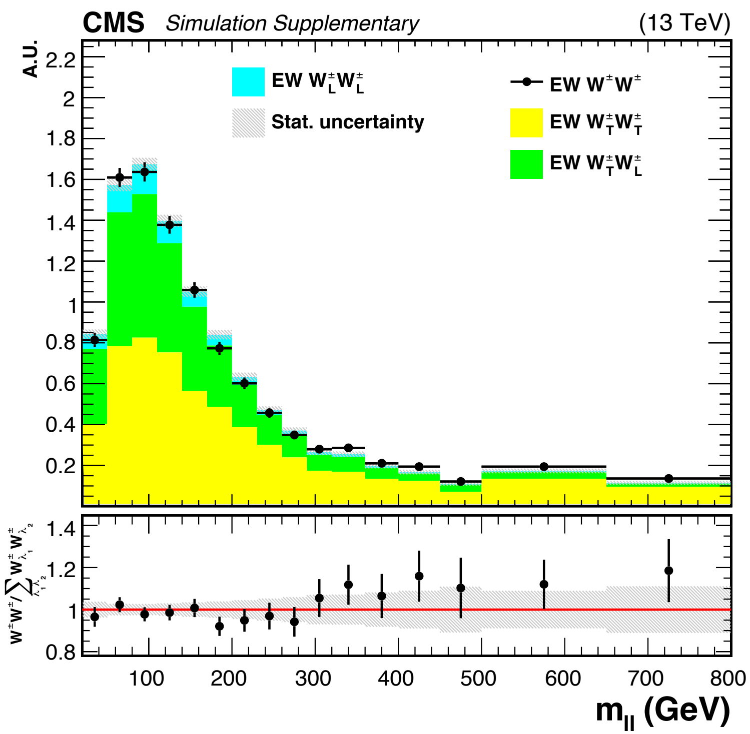

pp CM

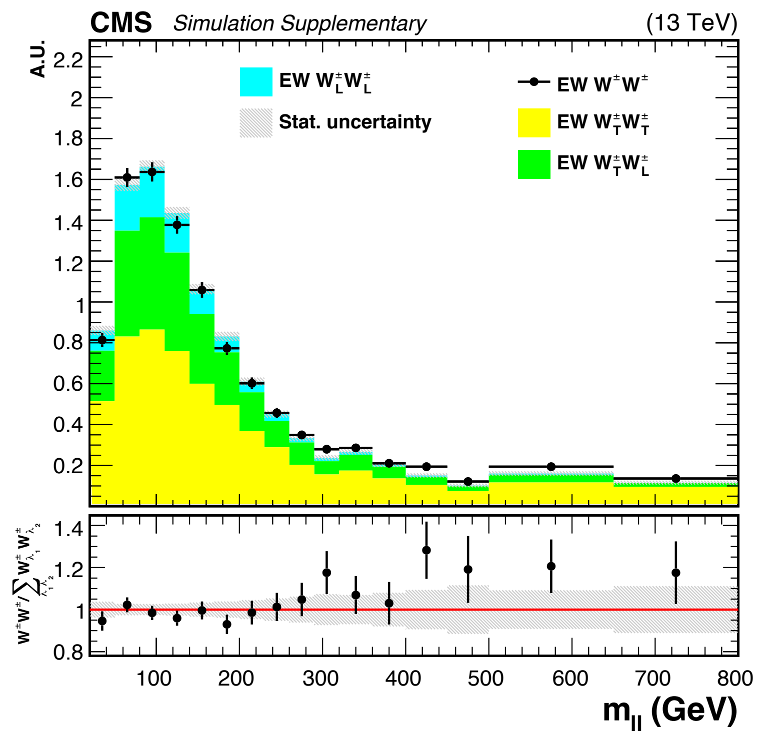

WW CM

Charged Higgs searches

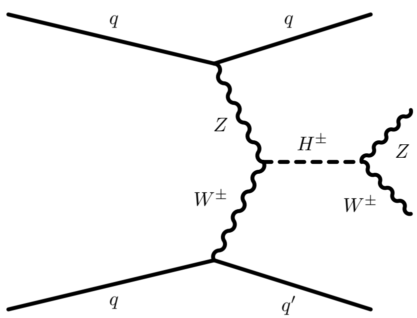

- How about Higgs triplet models?
- Two hallmark signatures of T=1
  - Tree level H^{+} WZ coupling
  - Doubly charged higgs: H^{++}
- We want to preserve the custodial symmetry
- Georgi-Machacek model: Doublet (T=1/2,Y=1), one triplet (T=1,Y=0), and one triplet with (T=1,Y=2)
  - Tree level custodial symmetry even with large contribution of vev carried by triplet sector!

$$\Phi = \begin{pmatrix} \phi_2^* & \phi_1 \\ -\phi_1^* & \phi_2 \end{pmatrix}, \qquad \Xi = \begin{pmatrix} \chi_3^* & \xi_1 & \chi_1 \\ -\chi_2^* & \xi_2 & \chi_2 \\ \chi_1^* & -\xi_1^* & \chi_3 \end{pmatrix}. \qquad \sin\theta_H =: s_H = \frac{2\sqrt{2}v_\Xi}{v_{\mathrm{SM}}}$$

  - Fermiophobic H^{++} and H^{+} produced via VBF

Same-sign WW

- $W^{\pm}W^{\pm}$ has the largest ratio of EW production to QCD initiated production
  - Double charge structure of the leptonic final state
  - QCD consists of diagrams with a gluon connecting the quark lines (no diagrams with gluon-gluon or quark-gluon)

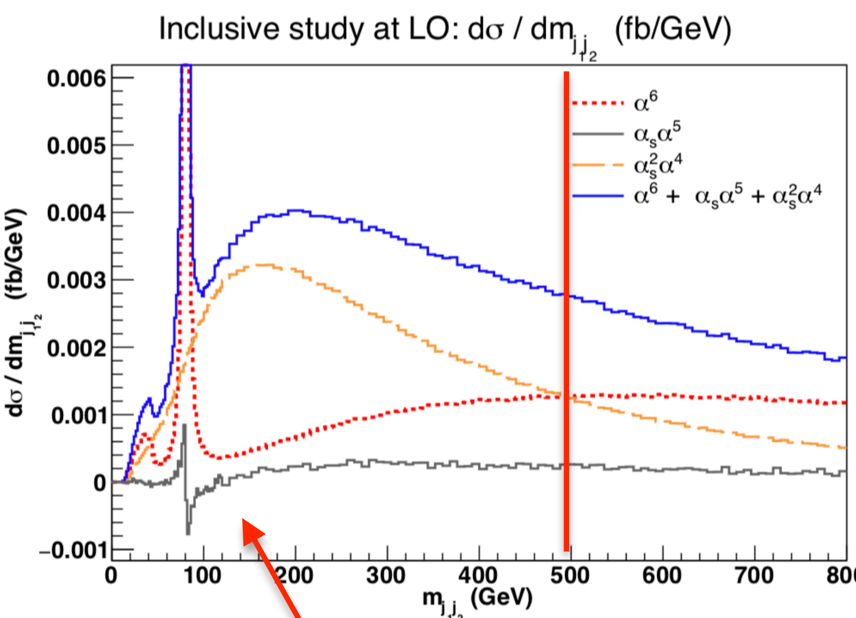

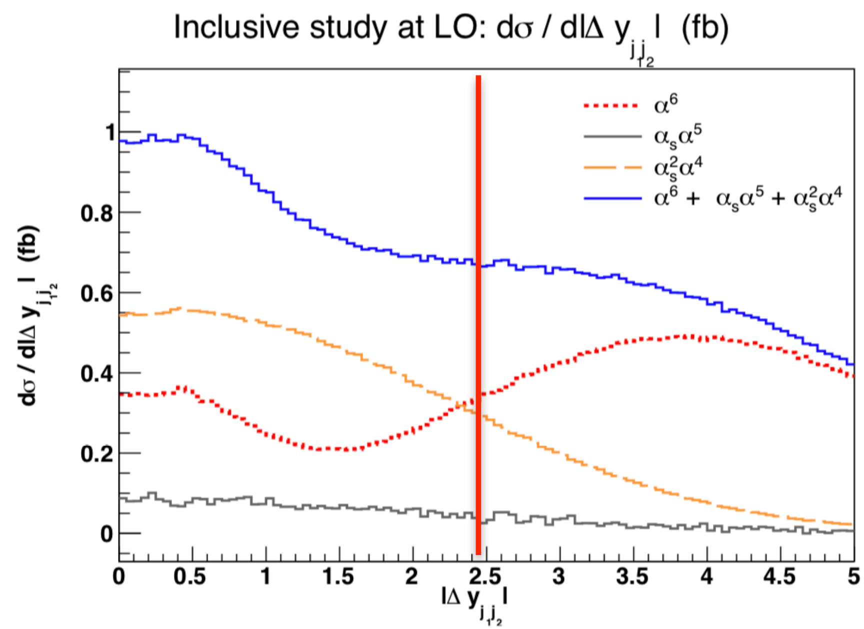

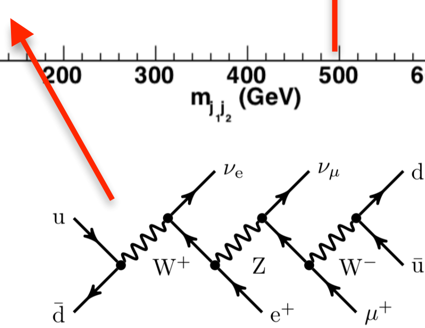

Ballestrero, et al.; 1803.07943

Experimental signature

- VBS events at LHC have distinct event topology
  - Two energetic jets with large di-jet mass (m_{jj}) and pseudorapidity separation $|\Delta y_{jj}|$
  - "Centrality" of the diboson system with respect to the two forward jets
- Common feature of all VBS signatures
  - Example of W^+W^+
- Cuts to enhance the EW contribution
  - m_{jj} and $|\Delta y_{jj}|$ requirements
  - 'Centrality' requirements

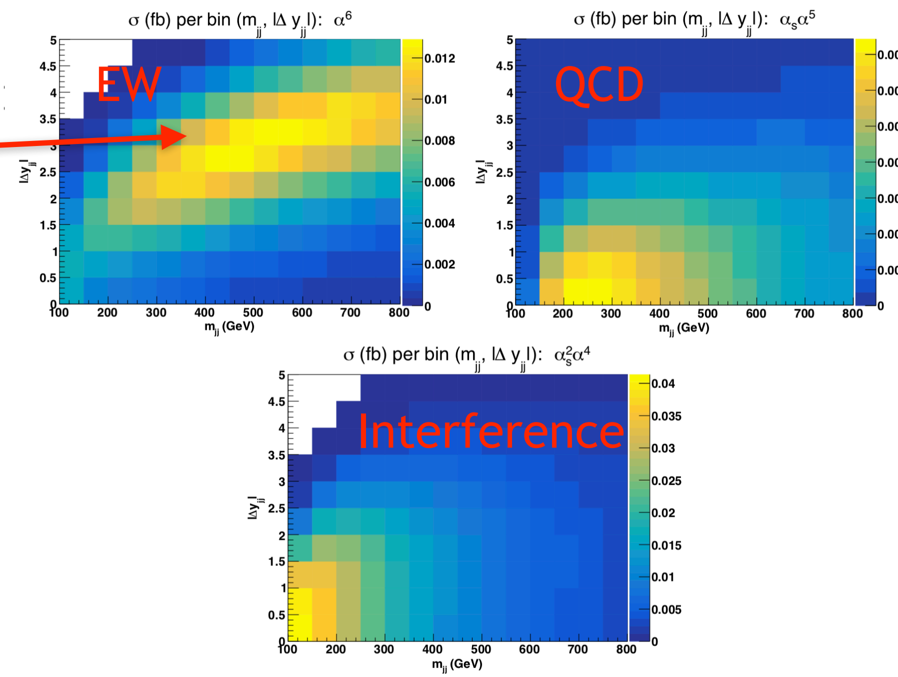

$$z_i = \frac{1}{\Delta\eta_{jj}}\left(\eta_i - \frac{\eta_1+\eta_2}{2}\right)$$

Phys. Rev. D 54 (1996) 6680

Ballestrero, et al.; 1803.07943

Large Hadron Collider

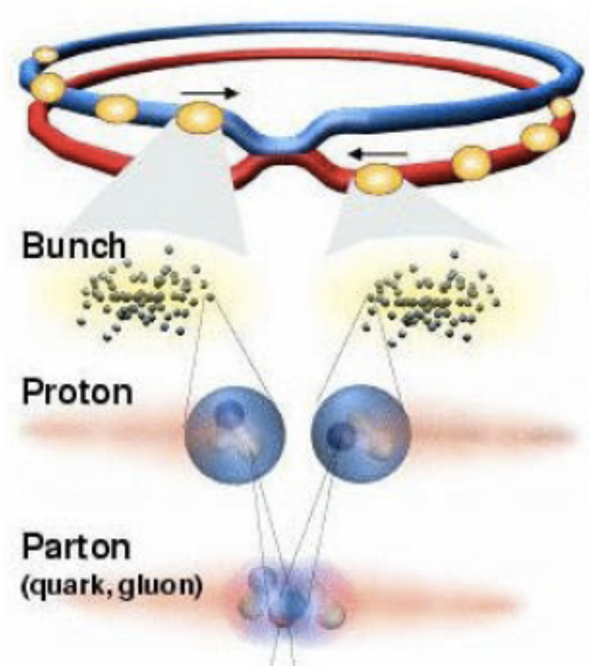

At least 10 orders of magnitude!

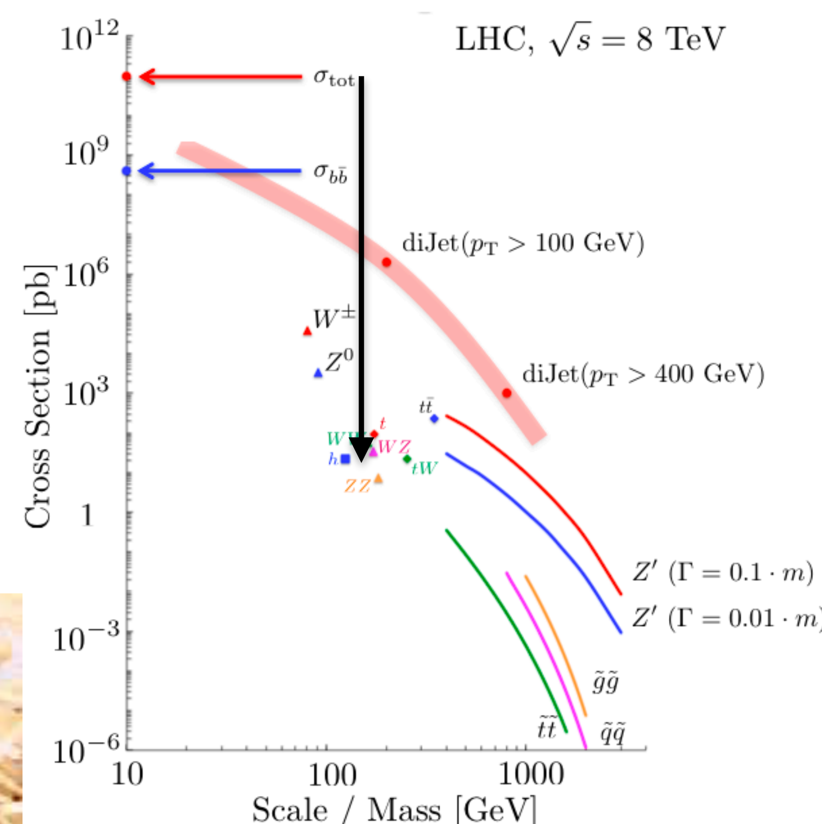

Standard Model of particles

- The 21st century picture of elementary particles

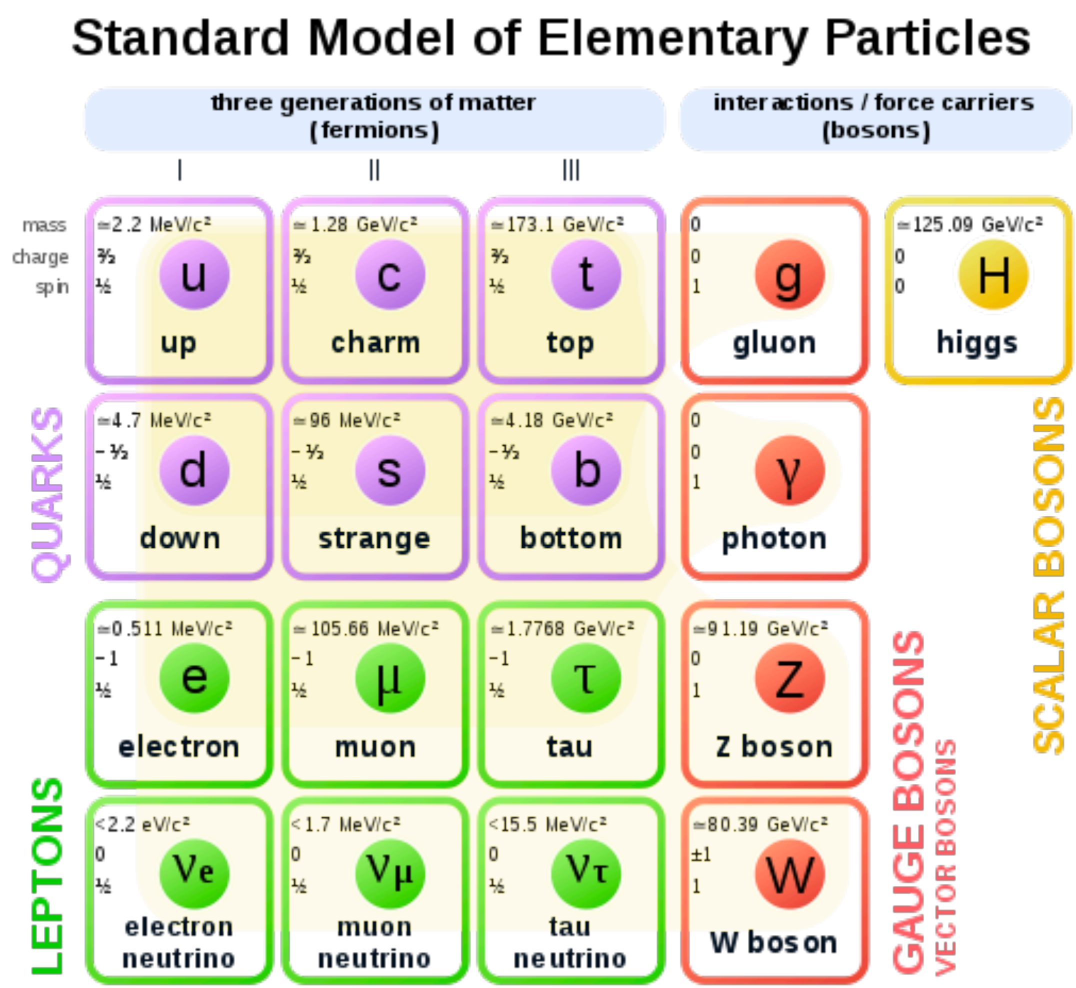

Large Hadron Collider

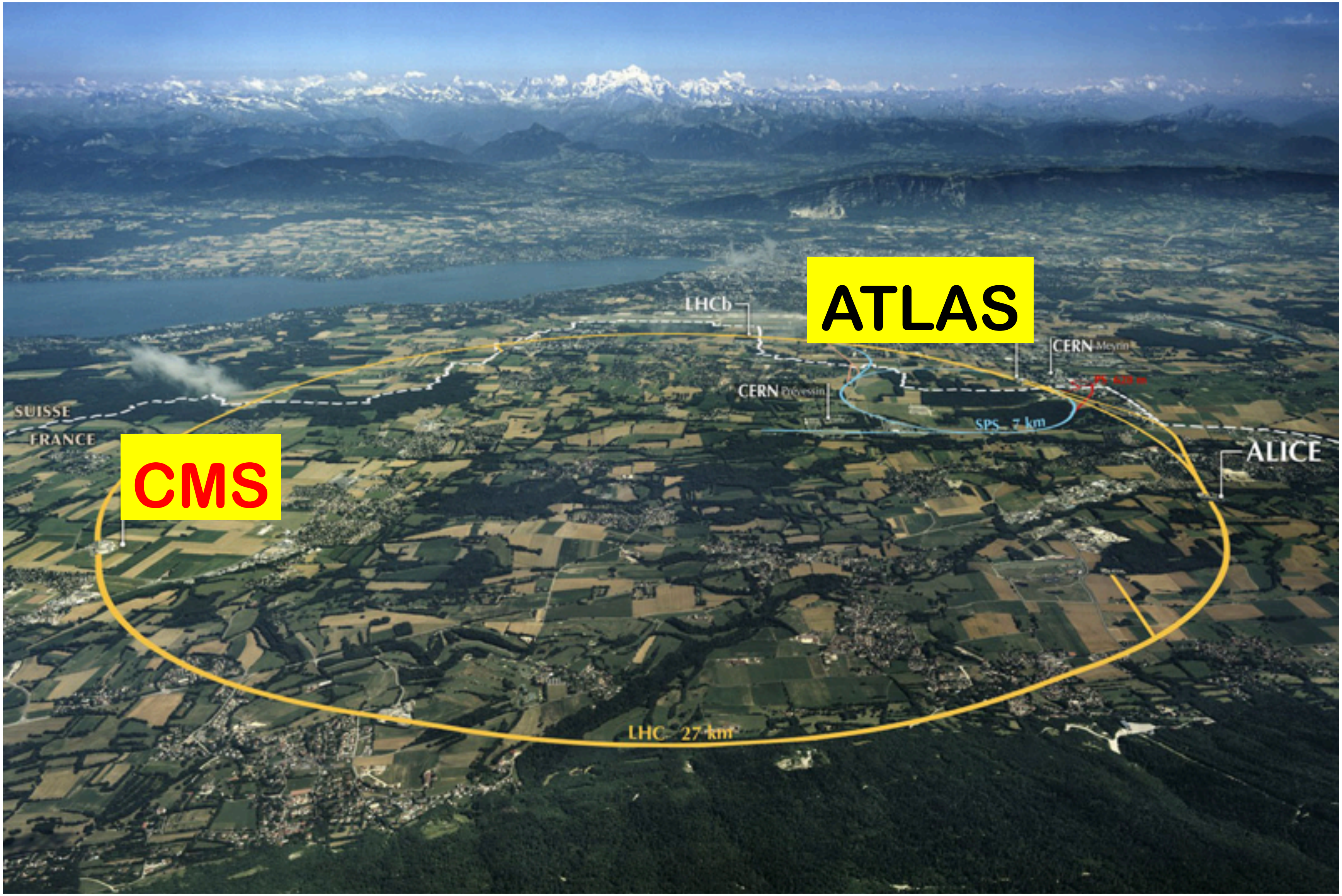

CMS detector

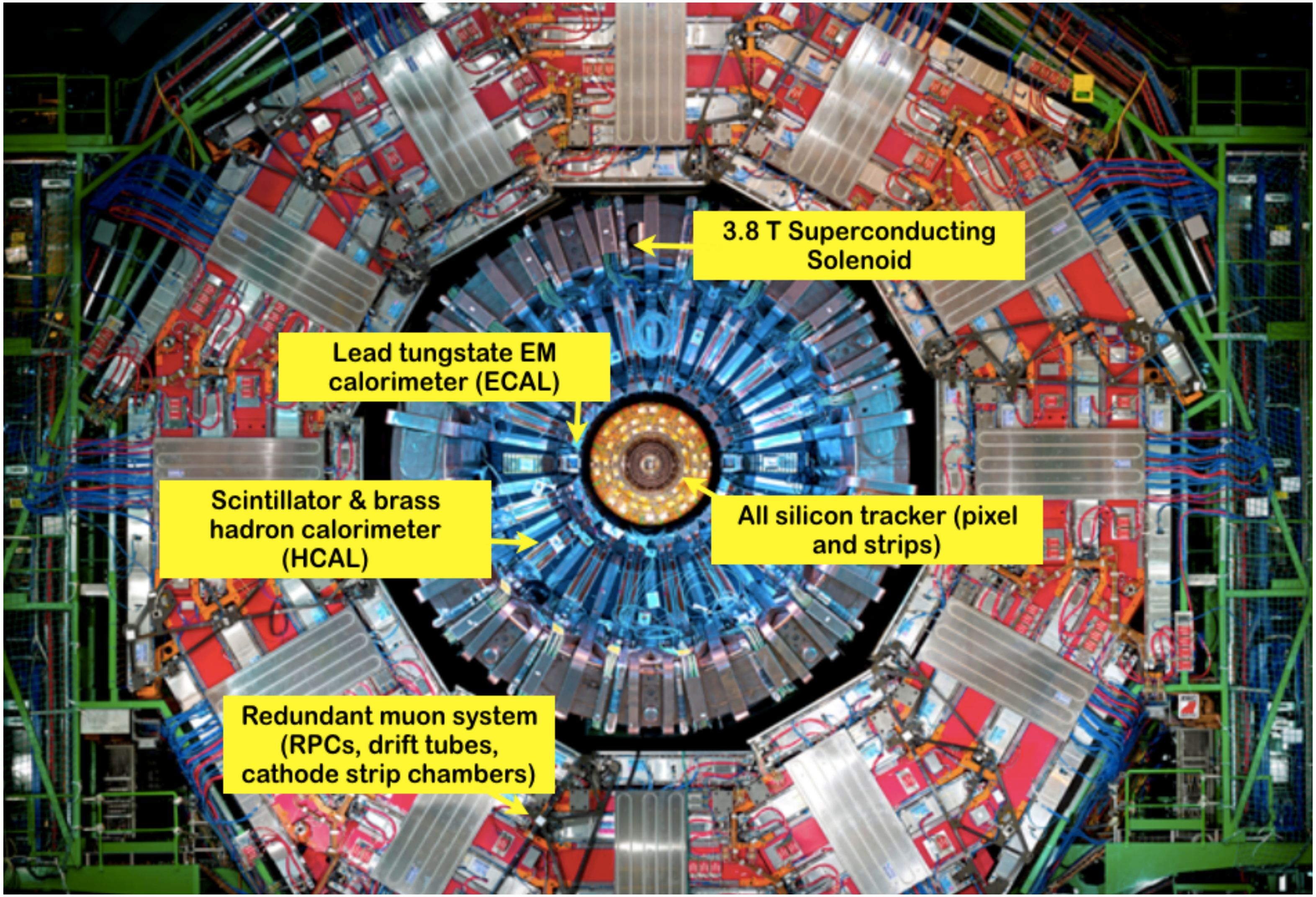

Enabling HL-LHC physics program

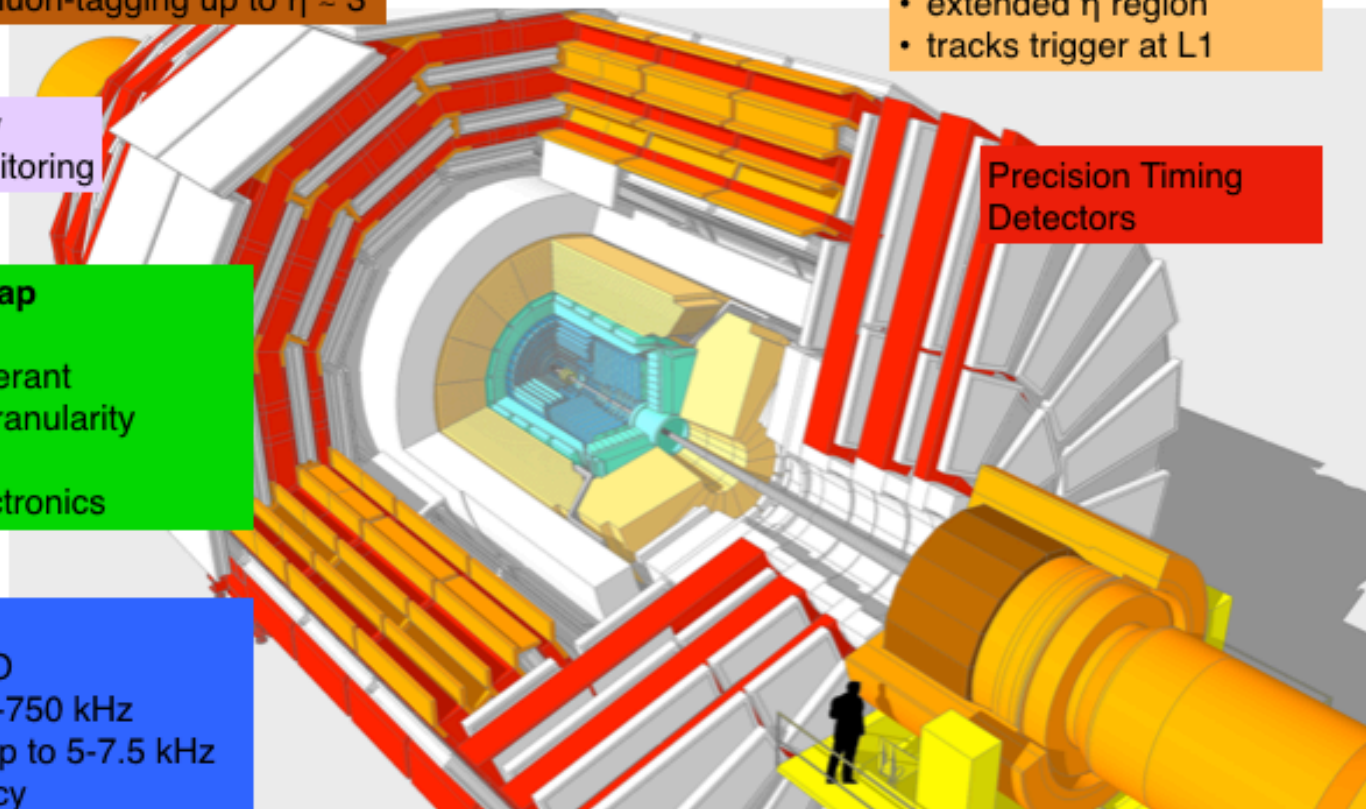

Muon System
- new DT FE electronics, CSC FEBs in inner rings
- extended η region (GEM & iRPC)
- investigate Muon-tagging up to η ~ 3

Tracker
- higher granularity
- less material
- better p_T resolution
- extended η region
- tracks trigger at L1

New luminosity and beam monitoring

Precision Timing Detectors

Replace Endcap Calorimeters
- radiation tolerant
- increased granularity

Barrel ECAL
- new FE electronics

Trigger/DAQ
- new FE & RO
- L1 up to 500-750 kHz
- HLT output up to 5-7.5 kHz
- 12.5µs latency
- tracking @L1